Fibonacci Fractal Tree Antennas

By

Başak ÖZBAKIŞ

**A Dissertation Submitted to the
Graduate School in Partial Fulfillment of the
Requirements for the Degree of**

MASTER OF SCIENCE

**Department: Electrical and Electronics Engineering
Major: Electronics and Communication**

**Izmir Institute of Technology
Izmir, Turkey**

July, 2004

We approve the thesis of **Başak ÖZBAKIŞ**

Date of Signature

…… **30.07.2004**

Assist. Prof. Dr. Alp KUŞTEPELİ
Supervisor
Department of Electrical and Electronics Engineering

……. **30.07.2004**

Assist. Prof. Dr. Thomas BECHTELER
Department of Electrical and Electronics Engineering

…….. **30.07.2004**

Assist. Prof. Dr. Yeşim YÜKSEL
Department of Electrical and Electronics Engineering
Dokuz Eylül University, İzmir

…….. **30.07.2004**

Prof. Dr. Ferit Acar SAVACI
Head of the Department of Electrical and Electronics Engineering

ACKNOWLEDGMENT

I would like to thank my supervisor Assist. Prof. Dr. Alp Kuştepeli for his support, guidance and great ideas. He never stops to trust me about doing the best.

I am very grateful to Assist. Prof. Dr. Thomas Bechteler for his comments and advice. I also thank Assist. Prof. Dr. Yeşim Yüksel for her support and encouragement.

I wish to express my thanks to the head of department Prof. Dr. F. Acar Savacı for his guidance to work on Fractal antennas. He always supported me about doing the best.

I would like to thank to my husband for his love and patience. He never stops to trust me. I am also very grateful to my family. They have always encouraged and supported me during my education. They always tell me to never stop learning.

ABSTRACT

Fractal geometry is first defined by Benoit Mandelbrot. A fractal structure is generated with an iterative procedure of a simple initiator by replicating many times at different scales, positions and directions. Fractal structures generated with this method are generally self-similar and the dimensions of these structures cannot be defined with integers. Koch, Minkowski and Sierpinski structures are the most known fractal structures. These structures are commonly used as multiband and wideband antenna designs because of the self-similarity. Furthermore, their special geometry is useful to obtain small antennas which are resonant at lower frequencies. Lowering the resonant frequency has the same effect as miniaturizing the antenna at a fixed resonant frequency.

Other important and interesting fractal structures used in antenna designs are the various types of the fractal trees. However, in recent studies the branch length ratios of the fractal tree antennas are taken constant. In this study fractal tree antennas with nonuniform branch length ratios are investigated. By changing the geometry and number of branches of the fractal tree structures the antenna characteristics are examined. The branch lengths and number of branches of the fractal tree antennas are determined by using the Fibonacci sequence. Leonardo Fibonacci (~1170 - ~1240), a famous Italian mathematician, dealt with geometry and developed a number sequence while observing the nature. Fractal tree antennas are designed with two different geometries in order to improve the resonance behavior of the antennas. The number of branches is decreased, so that less complex fractal tree antennas with the similar performance can be obtained.

ÖZ

Fraktal geometri ilk olarak Benoit Mandelbrot tarafından tanımlanmıştır. Fraktal bir yapı, basit bir geometriye sahip olan bir şeklin, defalarca farklı pozisyonlarda ve yönlerde kendini tekrarlamasıyla oluşur. Bu yöntemle oluşturulan fraktal yapılar genel olarak kendine benzer yapılardır ve bu yapıların boyutları tamsayılarla ifade edilemez. Koch, Minkowski ve Sierpinski, en çok bilinen fraktal yapılardır. Bu tip yapıların kendine benzer olması çok ve geniş bantlı anten tasarımlarında yaygın olarak kullanılmalarına olanak sağlamıştır. Ayrıca, özel geometrileri, düşük frekanslarda rezonansa girebilen küçük antenlerin elde edilmesinde faydalıdır. Rezonans frekansının düşmesi, sabit bir rezonans frekansında antenin küçülmesiyle aynı etkiye sahiptir.

Değişik tiplerdeki fraktal ağaçlar anten tasarımlarında kullanılan diğer önemli ve ilginç fraktal yapılardır. Fakat son zamanlardaki çalışmalarda fraktal ağaç antenlerin dal uzunluk oranları sabit alınmıştır. Bu çalışmada ise, dal uzunluk oranları sabit olmayan fraktal ağaç antenler incelenmiştir. Fraktal ağaç yapılarının geometrisi ve dal sayıları değiştirilerek anten karakteristikleri incelenmiştir. Fraktal ağaç antenlerin dal uzunlukları Fibonacci sayı dizisi kullanılarak elde edilmiştir. Ünlü bir İtalyan matematikçi olan Leonardo Fibonacci (1170 - 1240 civarı), geometri ile ilgilenmiş ve doğayı gözlemlemesi sonucu sayı dizisi geliştirmiştir. Antenlerin rezonans frekansını iyileştirebilmek amacıyla iki farklı geometriye sahip fraktal yapıda ağaç antenler tasarlanmıştır. Bunun yanı sıra benzer performansa sahip daha basit yapıda fraktal ağaç antenler elde etmek için dal sayıları azaltılmıştır.

TABLE OF CONTENTS

LIST OF FIGURES

LIST OF TABLES

Chapter 1

INTRODUCTION

Fractal geometry is defined by Benoit Mandelbrot in order to classify the structures, whose dimensions were not an integer [1]. Fractal structures have different geometrical properties than Euclidean structures. They are generated with an iterative procedure. In this procedure an initial structure called generator is copied many times at different scales, positions and directions [2]. Resulting structures are fine structures, and very detailed on small scales. They are irregular and cannot be described with traditional geometrical approaches. Fractals can have self-similar or similar forms and their fractal dimension can be greater than their topological dimension [3].

Many complex shapes found in nature can be formed with fractal geometry, such as clouds, mountains, coastlines and trees. Some examples for these complex shapes are given in Figure 1.1.

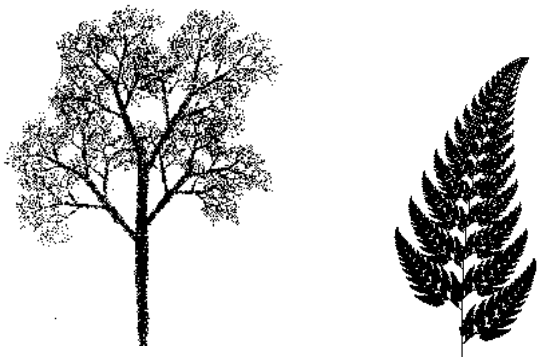

(a) (b)

Figure 1.1 Examples of fractal geometry found in nature: (a) Tree (b) Fern.

The tree shown in Figure 1.1a has a fine structure and it is irregular. The fern given in Figure 1.1b has a self-similar form. It means that it contains copies of itself at many scales.

Fractal geometries have been recently used in antenna designs in order to obtain small and miniaturized antennas, which have lower resonance frequencies. Koch curves, Koch and Minkowski loops are used as fractal structures in [4] and [5] to decrease the resonance frequency. In the analysis, lowering the resonance frequency has the same effect as miniaturizing the antenna at a fixed resonant frequency. Therefore, examining

the shift in the resonance frequency gives a good information about the miniaturization effect of the antenna. They are self-similar structures, so their scaled versions have same characteristics with the whole object. These fractal antennas can be used as wideband or multiband antenna. Additionally, fractal element antennas, including fractal loops, fractal dipoles and multiband fractal antennas, enhance miniaturization and other properties, making them suitable for a variety of many applications [6].

The factors affecting the antenna resonance characteristic have been discussed in [4-7]. It was given that there is a relation between the properties of the fractal geometry and the electromagnetic behaviour of an antenna. With respect to this relation it can be said that some fractals can be used in multiband antenna designs because of their self-similarity. The Sierpinski fractal antenna, which is investigated in [8] and [9], has similar performance at various frequencies. In these studies, the characteristic scale factor of the Sierpinski antenna is taken to be 1/2. However in the next studies the scale factor of the Sierpinski antenna is perturbed and it is observed that the radiating bands are shifted according to this perturbed scale factor [10-11].

A thin wire structure based on a fractal tree is investigated in order to find the wire equivalent model of the Sierpinski monopole patch antenna [12]. The tree was called a ternary fractal tree. Even though this antenna doesn't behave as efficiently as a multiband antenna, it can be used in the design of multiband electromagnetic filters or absorbers. The significance of the self similar fractal geometry in determining the multiband behavior of the Sierpinski antenna is discussed in [13]. It is analyzed that the multiband behavior of the Sierpinski gasket is primarily a function of the periodic placement of the four gaps located along the central vertical axis of the antenna. In the study [14] the height of the Sierpinski monopole is reduced by using Koch island loop as initiator. On the other hand, the multiband properties and the main cuts of the radiation patterns of this pre-fractal monopole doesn't change by reducing the height of the antenna.

Another fractal structure with a denser distribution is investigated in [15]. The antenna has many resonance frequencies because of its denser tree configuration.

Other fractal structures can exhibit multiband behavior. The multiband behavior of a fractal structure with various dimensions have been investigated and evaluated in [16]. The multiband behaviors of the Koch fractal monopole antennas generated with meander lines have been investigated in [17]. The Koch fractals are generated with meander lines and the multiband behavior of this pre-fractal is compared with the

original Koch curve. Both kinds of antennas show multiband behavior. Additionally, it can be said that antennas can show similar multiband behavior independent of differences in the antenna geometry and total wire length.

The significance of fractal structures in determining the resonant behavior is given in [18]. The performance of the Koch and Minkowski fractal antennas has been compared with non-Euclidean antennas. Both antennas have same performance. However the fractal structures of the non-Euclidean antennas in this study cannot be represented with Koch and Minkowski structures. These non-Euclidean structures aren't generators for the fractal structures Koch and Minkowski. Many antennas can be given as examples which show the same performance as Koch and Minkowski fractal antennas, but the comparison of the antennas' performance should be made with similar antenna structures to decide which antenna is better.

In study [19] it is given the space-filling ability of the fractal curves is affecting the resonance frequency whether or not. The performance of the Hilbert fractal curves are compared with meander line dipole antennas. It is given that the space filling ability cannot be the unique factor that affects the resonance frequency of the antennas.

The fractal dimension is another important parameter in the antenna designs [20]. The fractal dimension can be affected from the scale factor and the geometry of the antenna, however the form of the fractal structure is important [21]. If the fractal structure is self-similar then the similarity dimension is used, which is calculated with the number of copies and the scale factor of the antenna. Hausdorff dimension is a general formula to find the dimension of an antenna. The increase of fractal dimension of self-resonant fractal antenna does not improve its performance against Euclidean antennas in terms of radiation efficiency and quality factors [22-23].

Some pre-fractal monopole antennas have been investigated in [24]. The antennas can be miniaturized with using fractal geometry in antenna configuration. As explained in [24] the quality factor of the pre-fractal should be in lower values and radiation efficiency should have higher values when compared with the standard monopole antennas.

A simple straight wire has been analyzed long time ago in [25]. The performance of the straight dipole antenna is investigated in this study. Many two and three-dimensional fractal tree antennas have been recently used in the antenna designs. These fractal trees have similar forms and usually uniform branch length ratios. Various fractal tree antennas are designed to reduce the height of the dipole and monopole antennas.

The branch lengths of the fractal tree antennas are increasing according to the number sequence 1, 2, 4, 8, 16, 32, … from the tip of the antenna to the base and the branch length ratio is 1/2 [4]. The use of fractal tree configurations in antenna designs leads lower resonance frequencies than monopole antennas.

In many fractal tree antenna designs the branch length ratios have been taken uniform. In this study, 2D fractal tree antennas with nonuniform branch length ratios are investigated. The Fibonacci number sequence is used in determining branch lengths, which results nonuniform branch length ratios. The Fibonacci number sequence is developed by Leonardo Fibonacci [26]. In Chapter 2, the Fibonacci number sequence is explained in detail. Fractal tree antennas are simulated by using SuperNEC 2.7 [27]. SuperNEC uses Moment method for the calculations of the antenna parameters, such as input impedance, return loss, radiation pattern. In Chapter 3, the Moment method is investigated. Furthermore, fractal tree antennas with different branch length ratios are designed and analyzed in Chapter 4. Furthermore fractal tree configurations are changed by modifying the Fibonacci number sequence and the geometry of the branches. In Chapter 5, it is tried to improve the resonance behavior by changing the geometry of the tree branches. In order to reduce the complexity of the fractal tree antennas, the numbers of branches is changed according to the Fibonacci number sequence. In Chapter 6, the simulation solutions of the fractal tree antennas with different geometries are compared each other. The multiband behavior of the fifth iteration of the fractal tree antennas are examined in Chapter 7. Some applications for fractal antennas are given in Chapter 8. Finally, the conclusion is constituted according to the simulation results of the fractal tree antennas.

Chapter 2

FIBONACCI NUMBER SEQUENCE

Leonard Fibonacci (~1170 - ~1240), also called Leonard Pisano or Leonard of Pisa, was one of the most outstanding mathematicians of the European Middle Ages [26]. He wrote books about numeration system, arithmetic algorithms, geometry and trigonometri. “Liber Abaci” and “Practica Geometriae” (Practice Geometry) are some of his most famous books. Fibonacci employed algebra to solve geometric problems and geometry to solve algebraic problems. He dealt with many elementary problems. The rabbit population in a year is one of these problems, and it is explained numerically in his book “Liber Abaci”. He developed a number sequence while observing the rabbit population in one year. The original pair of rabbits was born in January 1. One month later they become mature, so there is one pair on February 1. On March 1 they are two months old and produce a new mixed pair, a total of two pairs. It continues like this and there are three pairs on April, five pairs on May, and so on. Hence, the pairs in rabbit population are increasing with the numbers 1, 1, 2, 3, 5, 8, 13, … in each month. This number sequence based on a recurrence algorithm, such as

$$F_n = F_{n-1} + F_{n-2}, \quad n > 2 \quad and \quad F_2 = F_1 = 1 \tag{2.1}$$

is called Fibonacci sequence. The amazing Fibonacci numbers appear in quite unexpected places in nature, such as in some spiral arrangements of the leaves on the twigs of plants and trees, on the mature sunflowers, on the petals of many flowers, on the pine cones, pineapples and artichokes. Additionally, many examples from plants can be given, in which Fibonacci sequence occurs. Sneezewort and Coltsfoot are special plants which include Fibonacci numbers in their body. In Figure 2.1, the sunflower is given as an example from nature.

Fibonacci number sequence occurs on the spiral numbers of the sunflower in the clockwise and counterclockwise direction.

Fibonacci numbers can be mathematically represented in many different ways. This special sequence is used in numerical applications. Several numerical identities of the Fibonacci numbers will be given in the next subsection.

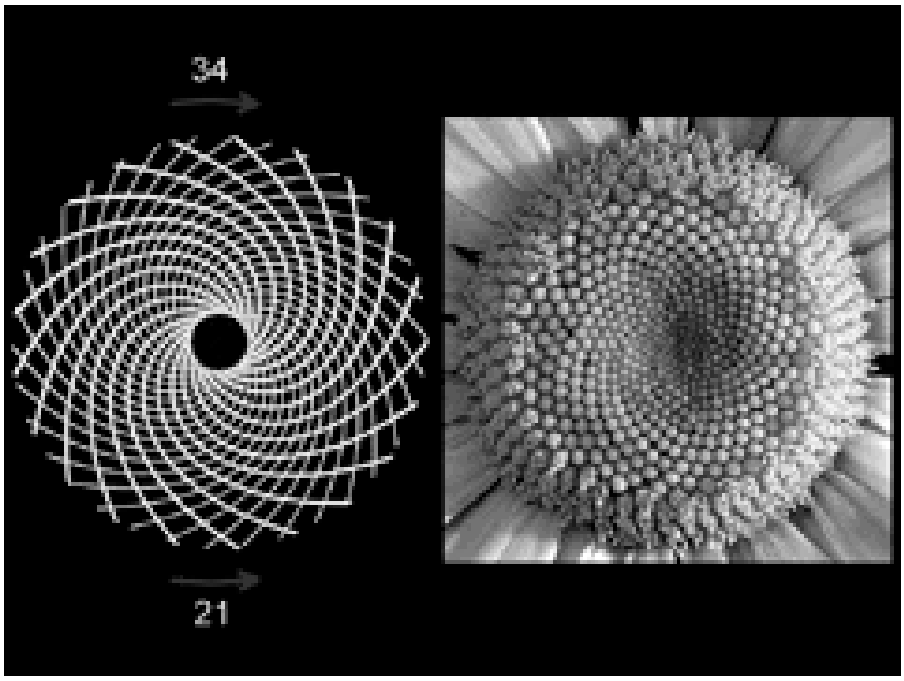

Figure 2.1 Fibonacci sequence in nature: sunflower.

2.1 Fibonacci Identity

The Fibonacci number sequence has different mathematical representations, which have been discovered over the centuries. For example a formula can be developed to find the sum of the Fibonacci numbers. The sum of the Fibonacci numbers can be found with a simple formula instead of summing the numbers step by step. In order to calculate the sum $\sum_{i=1}^{n} F_i$, the following interesting pattern can be constructed as

$$\begin{aligned} F_1 &= 1 = 2-1 = F_3 - 1 \\ F_1 + F_2 &= 2 = 3-1 = F_4 - 1 \\ F_1 + F_2 + F_3 &= 4 = 5-1 = F_5 - 1 \\ F_1 + F_2 + F_3 + F_4 &= 7 = 8-1 = F_6 - 1 \\ F_1 + F_2 + F_3 + F_4 + F_5 &= 12 = 13-1 = F_7 - 1. \end{aligned} \tag{2.2}$$

According to the above pattern $\sum_{i=1}^{n} F_i = F_{n+2} - 1$ can be obtained.

Another way of obtaining the sum is to write the Fibonacci numbers as

$$
\begin{aligned}
F_1 &= F_3 - F_2 \\
F_2 &= F_4 - F_3 \\
F_3 &= F_5 - F_4 \\
&\vdots \\
F_{n-1} &= F_{n+1} - F_n \\
F_n &= F_{n+2} - F_{n+1}.
\end{aligned} \tag{2.3}
$$

After adding these equations, we again get Eq.(2.3) as $\sum_{i=1}^{n} F_i = F_{n+2} - F_2 = F_{n+2} - 1$.

One of the most important relation between the numbers of Fibonacci sequence will be presented in the next subsection. The relation between the numbers of Fibonacci sequence will be observed in the next subsection. It is an interesting question whether the ratio of consecutive numbers of this special sequence converges to a number or not.

2.2 Golden Ratio

If the sequence of ratios $\frac{F_{n+1}}{F_n}$ of consecutive Fibonacci numbers is represented with a_n one can have

$$
a_n = \frac{F_{n+1}}{F_n} = \frac{F_n + F_{n-1}}{F_n} = 1 + \frac{F_{n-1}}{F_n} = 1 + \frac{1}{\frac{F_n}{F_{n-1}}} = 1 + \frac{1}{a_{n-1}} \ . \tag{2.4}
$$

If the limit can be obtained as the solution of the Equation (2.4) then the equation will be equal to

$$
x = 1 + \frac{1}{x} \tag{2.5}
$$

where

$$
x = \lim_{n \to \infty} a_n \ . \tag{2.6}
$$

By solving Equation (2.5), the roots are found as

$$x_{1,2} = \frac{1 \pm \sqrt{5}}{2}. \tag{2.7}$$

Since $F_n \geq 1$ and $F_{n+1}/F_n > 0$, the limit of the sequence a_n can't be a negative number. Therefore the positive root is the limit value. Then the limit is equal to the

$$\lim_{n\to\infty} \frac{F_{n+1}}{F_n} = \frac{1+\sqrt{5}}{2} = 1.618033... \tag{2.8}$$

and is called as the 'Golden ratio'. This ratio is used by Fibonacci to solve many geometric problems.

The Golden ratio can occur in extremely unlikely places such as several proportions of the human body, on many famous paintings. This ratio is used in engineering, mathematics, architecture, art and in music. Mimar Sinan, a famous architect, is used this special ratio in the minaret configurations of the Selimiye and the Süleymaniye mosques.

There are a lot of examples in mathematics and geometry. Golden triangles and golden rectangles are geometrical representations of the golden ratio and they are generated to solve some geometric problems. An isosceles triangle is a golden triangle if the ratio of one of its lateral sides to the base is nearly equal to the golden ratio. The top angle of the golden triangle is equal to the 36°. When a decagon (10-gon) is investigated, it is observed that each triangle in a regular decagon is a golden triangle. In addition to these geometric structures, it can be said that the pentagon contains golden triangles. In Figure 2.2 the golden triangle is shown.

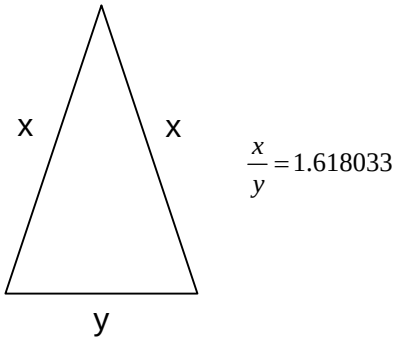

Figure 2.2 The golden triangle.

In the five pointed star the golden ratios can also be obtained [28]. As shown in Figure 2.3 the ratio of the distances *ab* and *ac* is equal to the golden ratio.

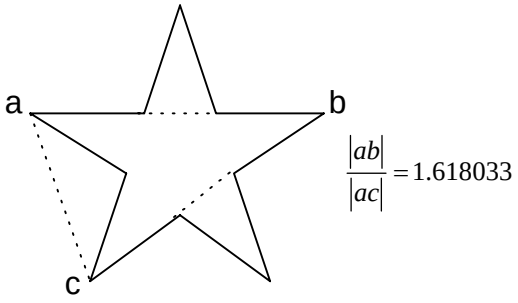

Figure 2.3 Five pointed star.

In Figure 2.4 a special rectangle can be examined, whose ratio of the length x of the longer side to the length y of the shorter side equals the ratio of their sum to the length of the longer side, that is

$$\frac{x}{y} = \frac{x+y}{x}. \tag{2.9}$$

and it is called golden rectangle.

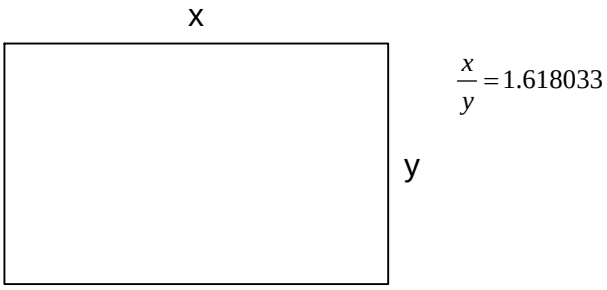

Figure 2.4 Golden rectangle.

Fibonacci numbers appear even in the study of electrical networks. In Figure 2.5, a ladder network with n equal resistors is shown. If this network is examined it is seen that the currents i_1 through i_n are proportional to 1, 1, 2, 3, 5, 8, 13, …, F_n, which are the sequential numbers of the Fibonacci sequence [28].

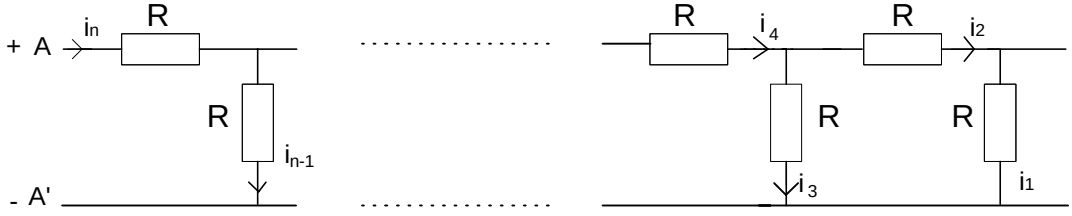

Figure 2.5 n ladder sections.

2.3 Outline of Work

The branch lengths of the fractal tree antennas are designed according to the Fibonacci number sequence from the tip of the antenna to the base in this study. The use of this special sequence in determining branch lengths leads to nonuniform branch length ratios in fractal tree antennas. The ratio of the consecutive branch lengths of these fractal tree antennas is equal to the 'Golden Ratio' while the iteration number goes to infinity.

The new tree is designed by leaving the first number out of the Fibonacci sequence. Then a similar algorithm is obtained with the previous recurrence algorithm, such as

$$F_{m_n} = F_{m_{n-1}} + F_{m_{n-2}}, \quad n > 2 \quad and \quad F_{m_2} = 2, \; F_{m_1} = 1. \tag{2.10}$$

The sequence 1, 2, 3, 5, 8, … is obtained according to the above algorithm and it is called modified Fibonacci sequence. Although the two algorithms are similar to each other, tree configurations are changing and different simulation results are obtained at lower iterations. Additionally, the branch lengths of the fractal tree antennas are increasing according to the modified Fibonacci sequence.

Another tree configuration is generated by changing the number of branches according to the modified Fibonacci sequence as shown in Figure 2.6 and called 'Dream tree.

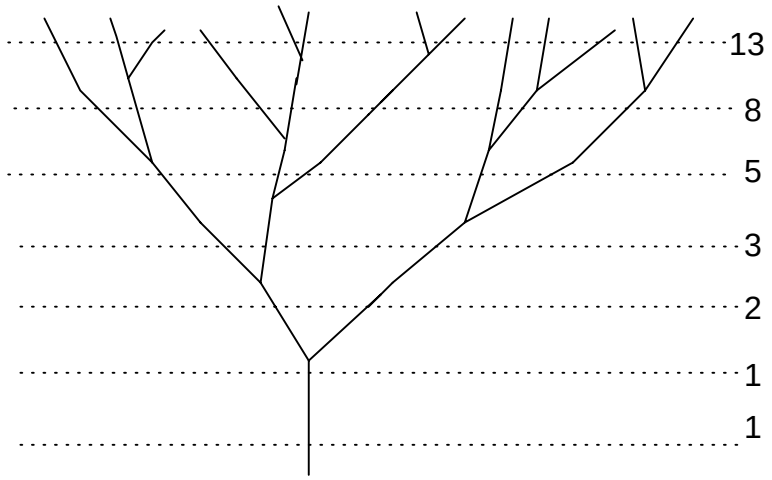

Figure 2.6 Dream Tree

The Dream tree presented in Figure 2.6 also shows the growth of the rabbit population mentioned in the beginning of this chapter.

Chapter 3

SIMULATION METHODS

SuperNEC 2.7 Academic version is used for the simulation of the fractal tree antennas [27]. SuperNEC is an object-oriented version of the FORTRAN program NEC-2 (Numerical Electromagnetic Code version 2). The basic idea for modelling antenna with the SuperNEC code is to use short and straight line segments. An antenna and any other conducting object in its vicinity that affect its performance can be modelled using those segments. Proper choice of the segments for an antenna model is the most critical step to achieving accurate results. Generally the segment length should be less than about one tenth of a wavelength at the frequency of operation and the model is analyzed by using the Moment of Methods.

3.1 Moment Method

The Moment method is a numerical technique for solving an integral equation obtained for the current density on the body of a structure [29]. In this study, perfectly conducting wires on an infinitely extending ground plane are simulated.

The moment method is employed by using the electrical field integral equation (EFIE) on perfect electrical conductors (PEC). The total electric field is obtained as

$$\boldsymbol{E}^{t} = \boldsymbol{E}^{\mathrm{i}} + \boldsymbol{E}^{\mathrm{s}} \tag{3.1}$$

and the boundary condition to be enforced on the PEC is

$$\hat{n} \times \boldsymbol{E}^{t} = 0 \tag{3.2}$$

The scattered field $\boldsymbol{E}^{s}$ can be obtained in terms of the magnetic vector potential **A** and the scalar electric potential Φ as

$$\boldsymbol{E}^{s} = -j\omega \boldsymbol{A}(\boldsymbol{r}) - \nabla\Phi \tag{3.3}$$

If the Equation 3.3 is substituted into Equation 3.2 then the Electric Field Integral Equation (EFIE) is found as

$$[-j\omega \boldsymbol{A}(r) - \nabla\Phi(r)]_{tan} = -\boldsymbol{E}^{i}_{\boldsymbol{tan}}(r) \tag{3.4}$$

where

$$\boldsymbol{A}(r) = \mu \int_S J(r')G(r,r')dS' \tag{3.5}$$

$$\Phi(r) = \frac{-1}{j\omega e}\int_S \nabla' \cdot J(r')G(r,r')dS' \tag{3.6}$$

$$G(r,r') = \frac{e^{-jkR}}{4\pi R} \tag{3.7}$$

and $\boldsymbol{R} = |\boldsymbol{r} - \boldsymbol{r}'|$ is the distance between the observation point r and the source point $\boldsymbol{r}'$ and $k=2\pi/\lambda$ with λ being the wavelength. The surface currents can be represented with a set of basis functions, f_n

$$J(r') = \sum_{n=1}^{N} I_n f_n(r') \tag{3.8}$$

where I_n are unknown current coefficients to be determined. After solving the current coefficients one can obtain the current by using the Equation (3.8).

Integrals are approximated by the sum of integrals over N small segments. When the antennas are fed with a voltage source, then the integral equation can be converted to a form such as

$$[Z][I] = [V] \tag{3.9}$$

and the unknown current coefficients can be obtained as

$$[I] = [Z]^{-1}[V]. \tag{3.10}$$

There are other factors that affect the solution in SuperNEC. The wire radius, ***a***, relative to the wavelength is limited by the approximations used in the kernel of electric

field equation. There are two approximation options available in SuperNEC. The first one is the thin wire kernel and the second is extended thin wire kernel. In the thin wire kernel, the current on the surface of a segment is reduced to a filament of current on the segment axis. In the extended thin-wire kernel, a current uniformly distributed around the surface of the segment is assumed.

The accuracy of the numerical solution also depends on the ratio of the segment length to the wire radius $(\Delta/\boldsymbol{a})$. Studies of the computed field on a segment due to its own current have shown that with the thin-wire kernel, $(\Delta/\boldsymbol{a})$ must be greater than about 8 for errors of less than 1%. For the extended thin wire kernel, $(\Delta/\boldsymbol{a})$ may be as small as 2 for the same accuracy. Reasonable current solutions have been obtained with the thin wire kernel for $(\Delta/\boldsymbol{a})$ down to about 2 and with the extended thin wire kernel for $(\Delta/\boldsymbol{a})$ down to 0.5. When a model includes segments with $(\Delta/\boldsymbol{a})$ less than about 2, the extended thin-wire kernel should be used.

3.2 Far field Calculations

The far field patterns of the fractal tree antennas are calculated with using standard far field approximations, such that

$$\boldsymbol{E} = -j\omega \boldsymbol{A}_T \tag{3.11}$$

$$\boldsymbol{H} = \frac{-j\omega}{\eta} \hat{r} \times \boldsymbol{A}_T \tag{3.12}$$

where A_T is the transverse component of the magnetic vector potential, ω is the angular frequency, $\eta = \sqrt{\frac{\mu}{\varepsilon}}$ and $\hat{r}$ is a unit vector in the observed direction of the far field such that

$$\hat{r} = \hat{x}\sin\theta\cos\varphi + \hat{y}\sin\theta\sin\varphi + \hat{z}\cos\theta. \tag{3.13}$$

The magnetic vector potential can be calculated as

$$\boldsymbol{A}(r) = \frac{\mu}{4\pi}\frac{e^{-jkr}}{r}\int_S J(r')e^{-jk\hat{r}\cdot\hat{r}'}dS' \tag{3.14}$$

Since the antenna surface is PEC there is no losses on the antenna, and the efficiency of the antenna is equal to 1. The directivity of the antenna is calculated with the ratio of the radiation intensity to the input power of the antenna.

$$D(\theta,\varphi) = 4\pi\frac{U(\theta,\varphi)}{P_{in}} \tag{3.15}$$

where

$$U(\theta,\varphi) = \frac{1}{2\eta}\left(\left|E_\theta(\theta,\varphi)\right|^2 + \left|E_\varphi(\theta,\varphi)\right|^2\right) \tag{3.16}$$

and

$$\boldsymbol{P_{in}} = \frac{1}{2}\mathrm{Re}(\boldsymbol{VI}^*) \tag{3.17}$$

As shown in Equation (3.16) the radiation intensity $U(\theta,\varphi)$ (W/unit solid angle), is a far field parameter and it can be calculated from both the polarization components of the scattered electric field. By examining the Equation (3.17) one can see that the power supplied to the antenna is computed from the applied voltage and computed current.

Chapter 4

FRACTAL TREE ANTENNAS

Fractal geometry is used in antenna designs in order to improve the resonance behavior of the antennas and to obtain smaller antennas that have lower resonance frequencies. When the resonance frequency for the antennas is set to be constant, the height of the fractal antennas becomes smaller than the standard monopole antennas. Hence lowering the resonance frequency has the same effect as miniaturizing an antenna at a fixed resonance frequency. In order to use small and efficient antennas instead of longer antennas, fractal tree structures are used in antenna designs, which provide to decrease the resonance frequency of the straight monopole or dipole.

In this chapter, the performance in decreasing resonance frequency of the similar fractal tree antenna structures is investigated. Fibonacci number sequence is used to design fractal tree antenna that has nonuniform branch length ratios. The performance of the fractal tree antennas are evaluated by means of the simulation results of the return loss, quality factor and system gain and the radiation patterns. The simulation results of the Fibonacci fractal tree antennas are compared with fractal tree antennas, which have uniform branch length ratios. The numerical computer simulation tool SuperNEC 2.7 is used for these investigations. [27].

4.1 *D (Double)* version Fractal Tree Antennas

The first fractal tree antenna is called *Double* version and the geometry of this fractal tree antenna feeding as a dipole is given in Figure 4.1.

The fractal tree antenna is generated by applying an iterative procedure to the generator monopole. At the first iteration, the top of the monopole is splitting with an angle 60° into two branches; one of the branches is splitting with an angle 60° through left, the other one is splitting in the same direction with the previous branch. The iterative process goes on to generate fractal tree antennas called *D* version. The antennas have closed structures like shown in Figure 4.2.

The branch lengths are increasing according to the number sequence 1, 2, 4, 8, 16, 32, …, from the tip of the antenna to the base. Therefore their branch length ratios are 1/2, and they have uniform branch length ratios. The ratio of the branch lengths to the total length is given in Table 4.1.

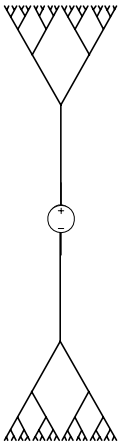

Figure 4.1 Geometry of the *D* version fractal tree dipole antenna.

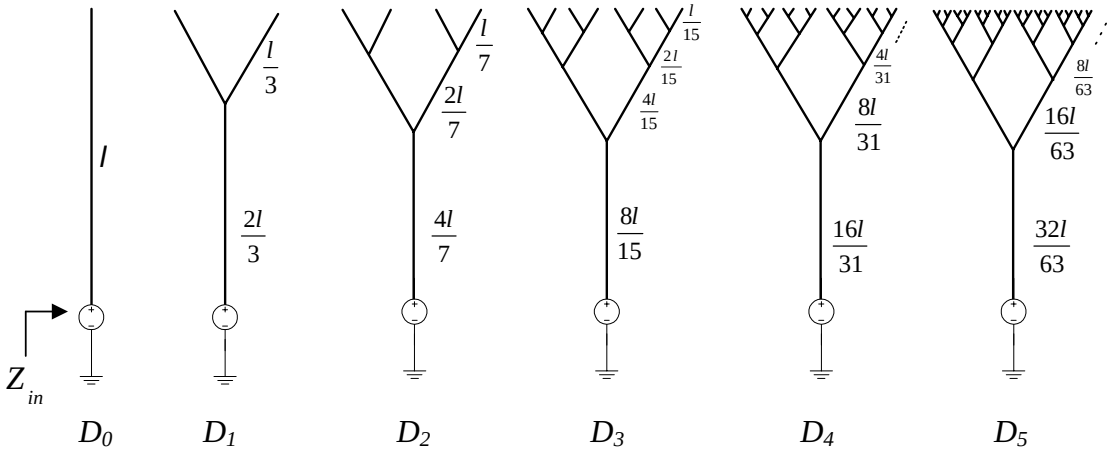

Figure 4.2 *D* version fractal tree monopole antenna configurations.

Table 4.1 Branch length ratios of *D* version fractal tree antennas.

iteration	0	1	2	3	4	5
Branch length ratios	1	1/3	1/7	1/15	1/31	1/63
		2/3	2/7	2/15	2/31	2/63
			4/7	4/15	4/31	4/63
				8/15	8/31	8/63
					16/31	16/63
						32/63

The length of the fractal tree antennas is 3.75 cm from the base to the tip of the last branches for all cases. The first five iterations and a straight monopole are analyzed. The antenna is fed at its bottom, which is connected to an infinitely extended ground plane. The radius of all wires is 0.0075cm and the wires are perfectly electrical conductors. The antenna is divided into 60 segments which correspond to a length *l*/60, where *l* is still the length of a path from the base to one tip of the antenna.

4.2 *F* (*Fibonacci*) version Fractal Tree Antennas

The special fractal tree antenna that is designed by using Fibonacci number sequence is called *F* version fractal tree antenna. The antenna is obtained in a similar way with the previous antenna, *D* version.

The angles between branches are 60°; one of them at each path is splitting with an angle 60° through the left or right, other one is splitting in the same direction with the previous branch. The five iterations of the *F* version fractal tree antenna with a straight monopole are given in Figure 4.3. The antennas have closed structures because of the geometry of the branches. The bottom part of the antennas is connected to an infinitely extending ground plane. All antennas are in same length, which is 3.75 cm. The radius of wires is 0.0075 cm. Each segment length is equal to the *l*/60 of the total length.

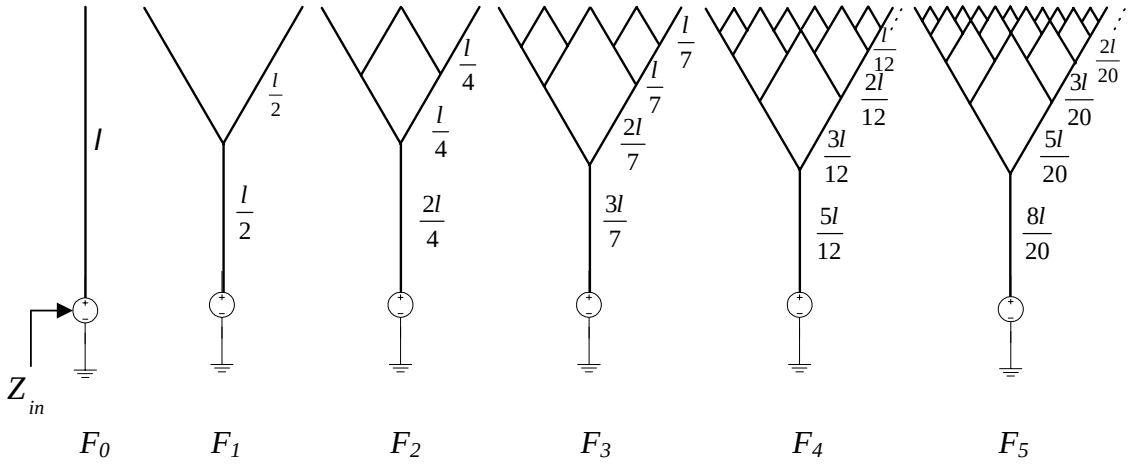

Figure 4.3 *F* version fractal tree configurations.

Some branches are touching each other at the tip of the antenna because of this special Fibonacci sequence. In this case the length of the branches is increasing from the tip to the base according to this special sequence. As shown in Table 4.2 the ratios of the branch lengths to the total lengths are nonuniform.

Table 4.2 Branch length ratios of *F* version fractal tree antennas.

iteration	0	1	2	3	4	5
Branch length ratios	1	1/2	1/4	1/7	1/12	1/20
		1/2	1/4	1/7	1/12	1/20
			2/4	2/7	2/12	2/20
				3/7	3/12	3/20
					5/12	5/20
						8/20

4.3 F_m (*modified Fibonacci*) version Fractal Tree Antennas

The branch lengths of the antennas are configured with using modified Fibonacci sequence and called F_m version. The initiator of this similar fractal geometry is monopole that is divided in two branches; one of the each branches is splitting with an angle 60° through left or right, the other stays in the same direction with the previous branch as shown in Figure 4.4.

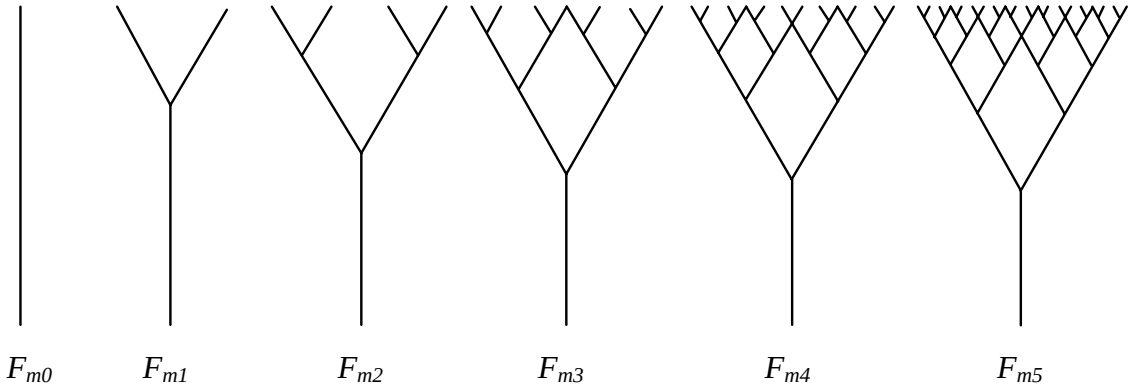

Figure 4.4 The configurations of the F_m version fractal tree antennas.

By examining Figure 4.4, one can see that there are some branches which are touching each other at the tip of the antenna. However, the number of touching wires in F_m version is less than those of the F version.

The antenna branch length ratios are nonuniform. In Table 4.3 the branch length ratios of the antennas are represented. The ratios are given from the tip of the antenna to the base.

Table 4.3 Branch length ratios of the F_m version fractal tree antennas.

iteration	0	1	2	3	4	5
Branch length ratios	1	1/3	1/6	1/11	1/19	1/32
		2/3	2/6	2/11	2/19	2/32
			3/6	3/11	3/19	3/32
				5/11	5/19	5/32
					8/19	8/32
						13/32

The monopole fractal antennas are fed at the bottom of the geometry and they are connected to an infinitely extending ground plane. The length of the antennas remains same in all cases and equal to the 3.75 cm from the base to the tip of the last

branches. The antennas are divided into 60 segments from the base to the tip. The radius of the wires is 0.0075 cm.

4.4 Results

Figure 4.5 shows the input reflection coefficients between 800 MHz and 2000 MHz. The index n=0, 1, 2, … at *D*, *F* and F_m designates the iteration. Hence, D_o, F_o and F_{mo} correspond to the standard monopole. The resonance frequencies of the fractal tree antennas are decreasing while the iteration number increases. With increasing iteration the effect of the frequency shift diminishes. The number of branches is increasing while the iteration number increases. This adds more conduction paths at the top of the antenna and it causes an increase in total conducting path lengths.

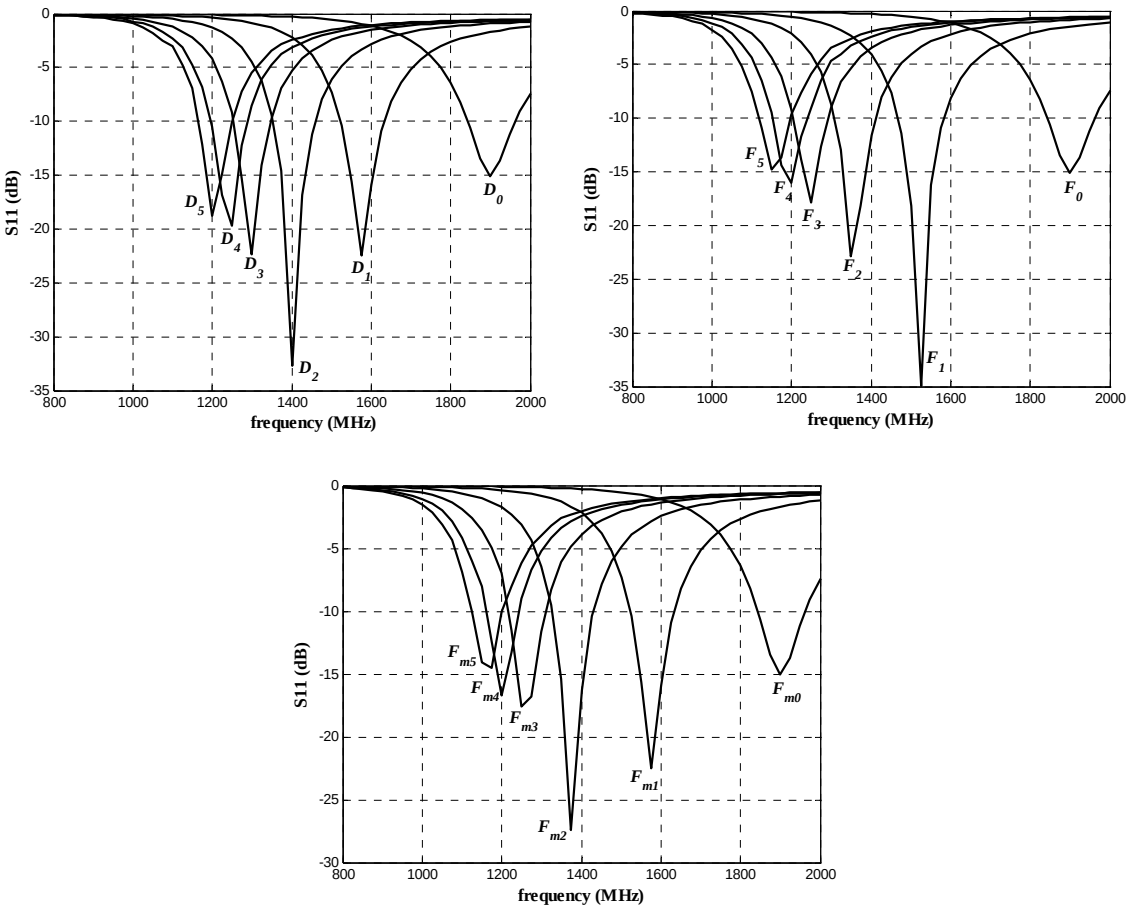

Figure 4.5 The input reflection coefficients of the *D*, *F* and F_m version fractal tree antennas.

The resonance frequencies of the F and F_m versions are closing each other while the iteration number increases. However their resonance frequencies are lower than the D version.

The resonance frequencies and the percent resonance frequency shifts of the proposed antennas, F and F_m with respect to the D version are given for each iteration in Table 4.4.

Table 4.4 The resonance frequencies* and the percent shifts of the closed structures.

Iteration	$f_{res,D}$	$f_{res,Fm}$	% Shift	$f_{res,F}$	% Shift
0	1900	1900	-	1900	-
1	1590	1590	-	1550	13
2	1400	1360	8	1350	10
3	1300	1255	7.5	1250	8.3
4	1245	1200	6.8	1195	7.6
5	1200	1158	6	1155	6.4

*****All resonance frequencies are given in MHz.

By examining the Table 4.4, one can see that the resonance frequencies are decreasing while the iteration number increases. F and F_m versions decrease the resonance frequency more than the D version for the same iteration. Furthermore, F_3 version can be used instead of D_4 version and F_4 and F_{m4} versions can be used instead of D_5 version, because these antennas have nearly same resonance frequencies.

The frequency shift is calculated by comparing the resonance frequency shifts of the F or F_m versions and the frequency shift of the D version with respect to the standard monopole. The resonance frequency shift in percent can be expressed as

$$\frac{f_{res,\,D\,i} - f_{res,\,f\,i}}{f_{res,\,sd} - f_{res,\,D\,i}} \tag{4.1}$$

where $f_{res,\,,D\,i}$ is the resonance frequency of the D version for the ith iteration, $f_{res,\,f\,i}$ is the resonance frequencies of the F and F_m version for the ith iteration, $f_{res,\,sd}$ is the resonance frequency of the standard monopole and is equal to 1900 MHz.

As shown in Table 4.4, the frequency shift of F and F_m versions is decreasing while the iteration number increases. The amount of frequency shift in percent of the F and F_m is at the same magnitude while the iteration number increases. It can be said that

the performance of the F and F_m versions in decreasing resonance frequency is similar at high iterations, since the antennas show nearly same resonance frequencies.

Figure 4.6 plots the resonance frequency of the D, F and F_m versions versus the iteration. F and F_m versions have nearly same resonance frequencies after the second iteration. As shown in Figure 4.6 the performance of the Fibonacci antennas in decreasing resonance frequency is better than the *D (Double)* version.

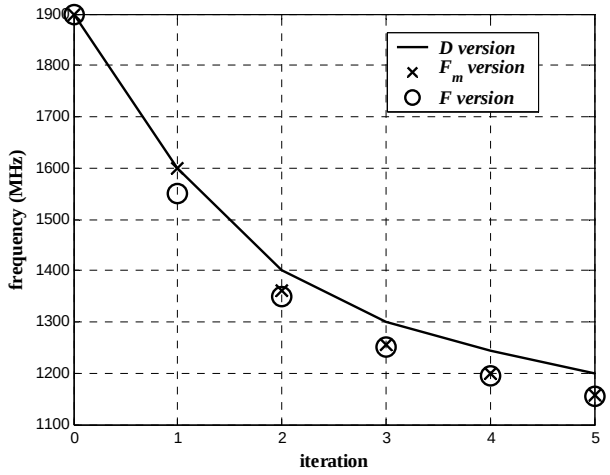

Figure 4.6 The comparisons of the antennas' resonance frequencies.

The input impedances of the antennas are measured using Moment Method mentioned in the previous chapter. The input impedance of the fractal tree antennas are decreasing while the iteration number increases. The input impedance of the D_5 is equal to 40Ω, while F_5 and F_{m5} have 34.6 Ω and 35.1 Ω input impedances.

Comparing the 3 dB bandwidths of D_5, F_5 and F_{m5} show that the bandwidths are very close. The F_{m5} version has a relative bandwidth of 24%, while D_5 and F_5 show relative bandwidths of 21% and 22% respectively.

The 10 dB bandwidths of D_5, F_5 and F_{m5} are about 6.6%.

The overall quality factor (Q) is defined as the ratio of the stored electric or magnetic energy, W_e and W_m respectively, to the radiated power P_{rad} and is given as

$$Q = \begin{cases} \dfrac{2\omega W_e}{P_{rad}}, & W_e > W_m \\ \dfrac{2\omega W_m}{P_{rad}}, & W_m > W_e \end{cases} . \qquad (4.2)$$

Q can be computed as

$$Q = \frac{\omega}{2R_{in}}\left(\frac{dX_{in}}{d\omega} + \left|\frac{X_{in}}{\omega}\right|\right) \tag{4.3}$$

where ω is the angular frequency and R_{in} and X_{in} are the input resistance and reactance of the antennas respectively [30-34]. The derivative of the input reactance can be obtained approximated by applying the central differences

$$\frac{dX_{in}}{d\omega} = \frac{X_{in}(freq_{n+1}) - X_{in}(freq_{n-1})}{freq(n+1) - freq(n-1)}, \quad n > 1 \tag{4.4}$$

in the numerical calculations [35]. As shown in Figure 4.7, the overall quality factors of the antennas are decreasing while the iteration number increases. The Q of the antennas are approaching to the fundamental limit of the antenna [36]. Fundamental limit for a small antennas can be calculated while ka=1, where k is the wave number associated with the electromagnetic field and a is the radius of a sphere which encloses the antenna.

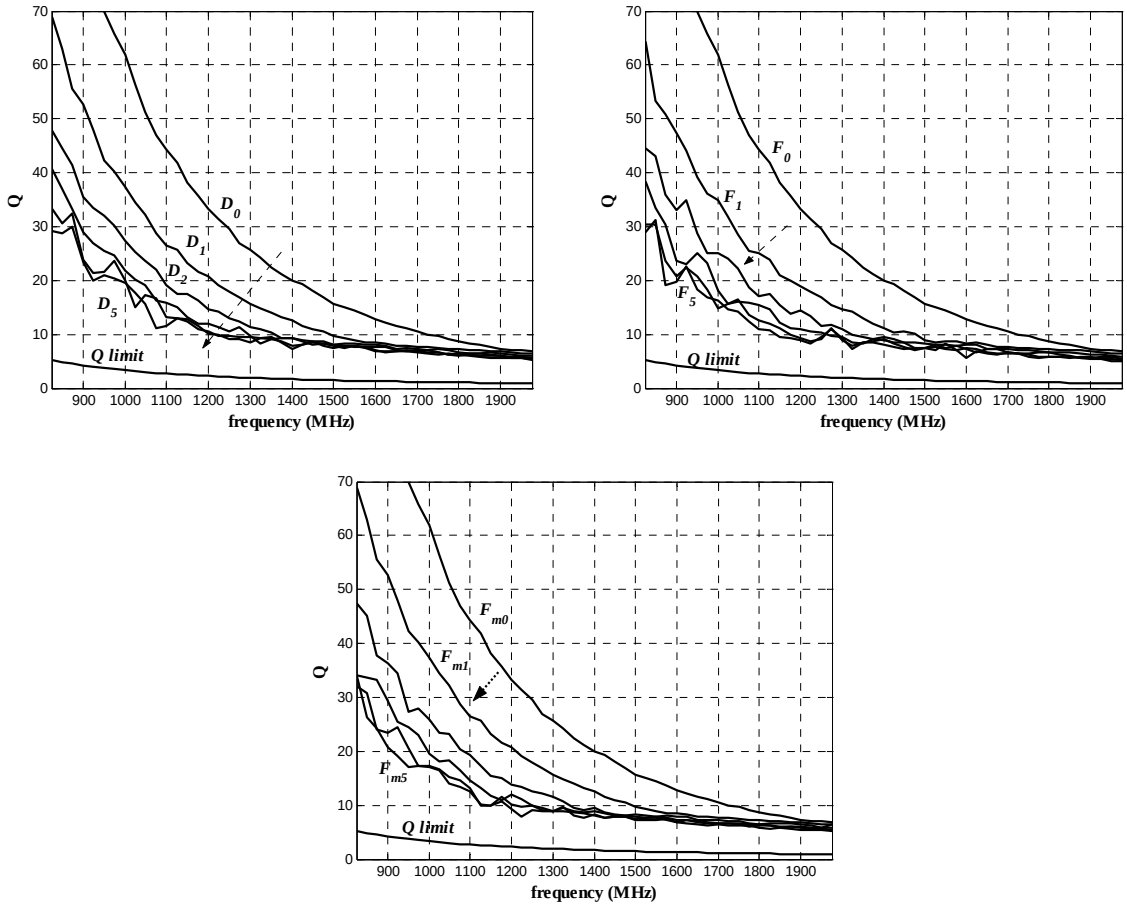

Figure 4.7 The overall quality factors of the *D, F* and F_m versions.

The overall system gain G_{sys} of the fractal tree antennas can be computed by using the formula

$$G_{sys}(dB) = G_A(dB) + 10\log(1 - |\Gamma|^2). \quad (4.5)$$

where G_A is the antenna gain and Γ is the reflection coefficient at the input of the antenna. The overall system gains of the antennas are shown in Figure 4.8. The overall system gains are shifting to the lower frequencies while the iteration number increases. Furthermore, tree antennas have same overall system gains. The antennas have maximum system gain at their resonance frequencies.

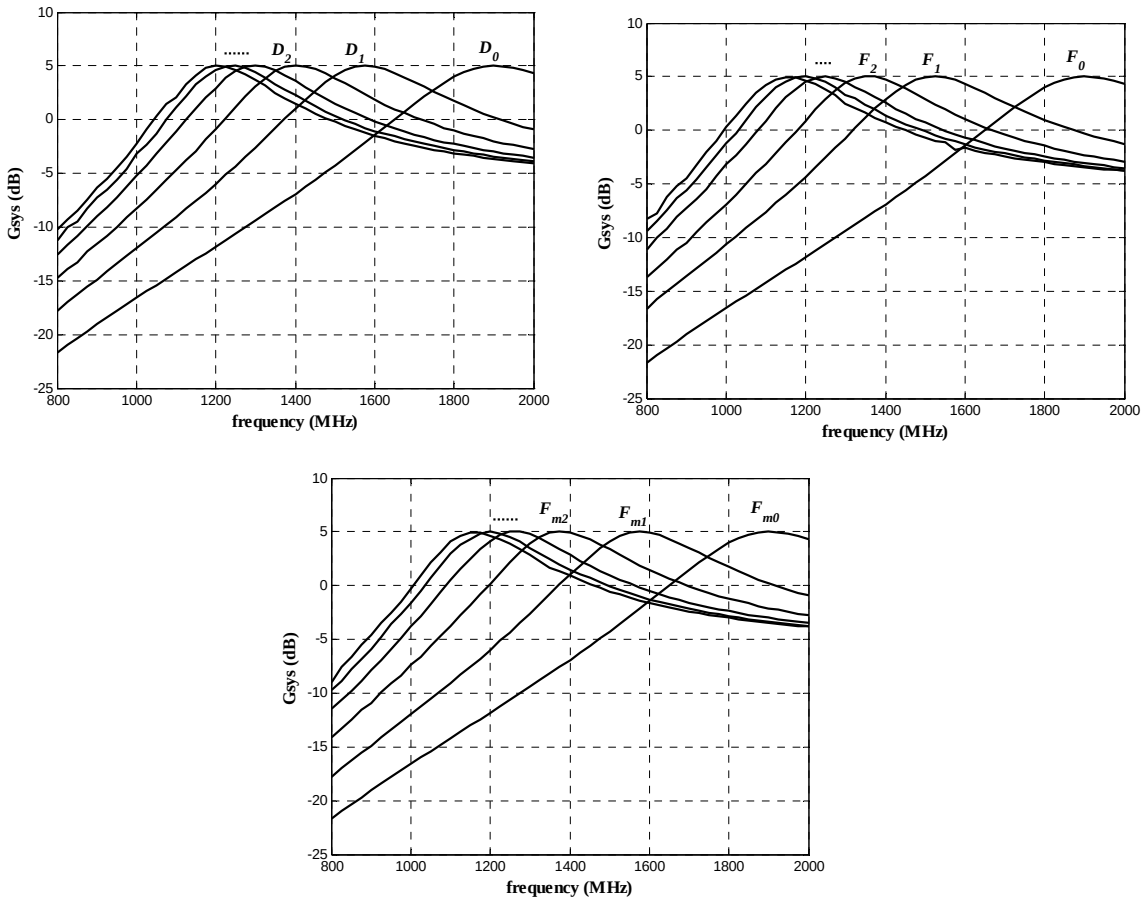

Figure 4.8 The simulated system gains of the fractal tree antennas versus frequency.

The radiation patterns of the D_5, F_5 and F_{m5} version fractal tree antennas at the first band frequencies are given in Figure 4.9. The patterns are similar with that of the standard monopole antennas. The polarization of the antennas is linear.

The fractal dimension of the tree antennas is calculated with a formula

$$\sum_{i=1}^{n} s_i^d = 1 \quad (4.6)$$

where i is the iteration number, s_i is the i^{th} iteration scale factor (or branch length ratio) and d is the fractal dimension. Total conducting path lengths of a fractal tree antenna can be calculated while the dimension is equal to 1. The dimensions of the D_5, F_5 and F_{m5} version fractal tree antennas are close to values 1.5, 1.67 and 1.65 respectively. while their total conducting path lengths are equal to 11.4 cm, 15.75 cm and 14.625 cm.

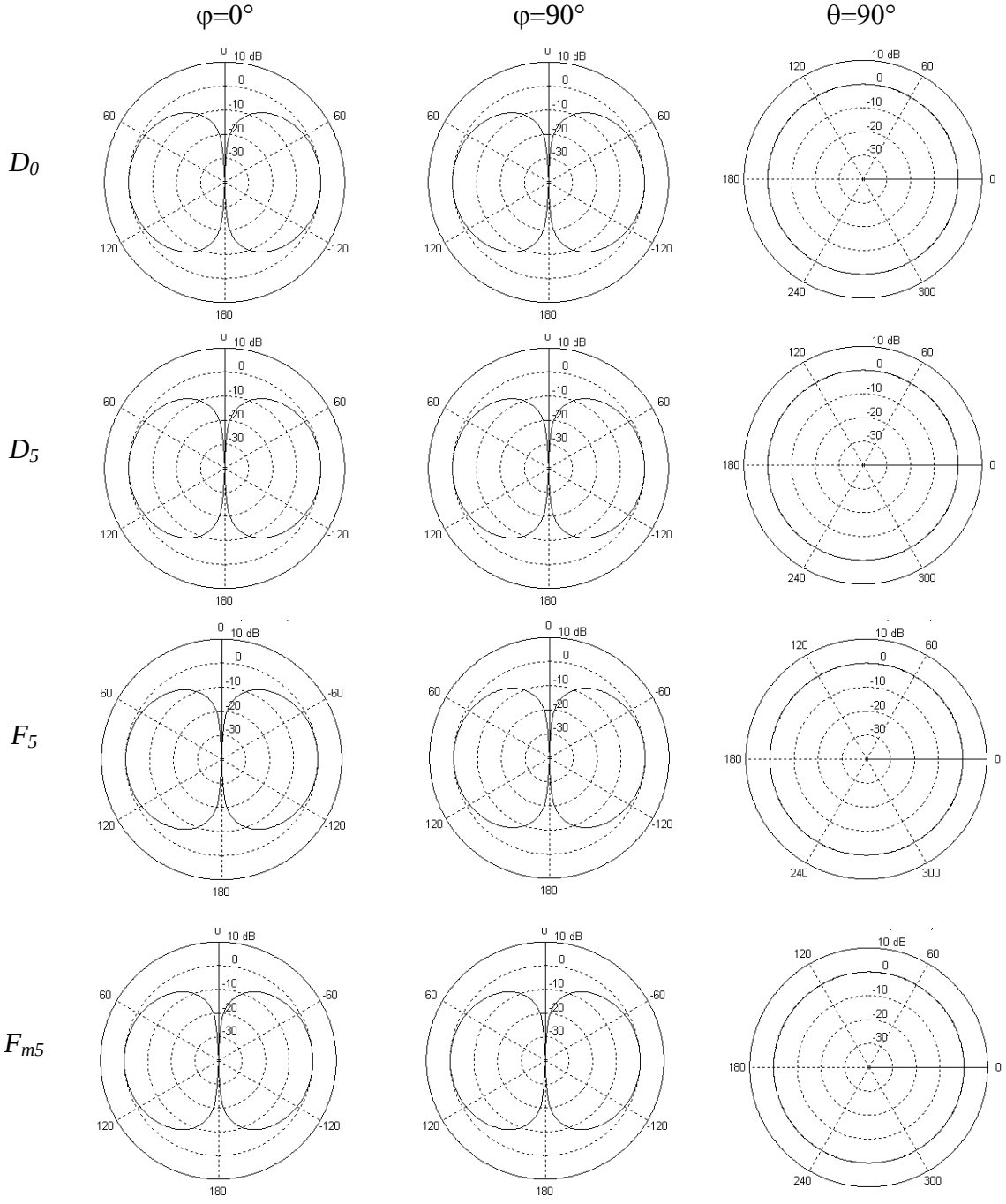

Figure 4.9 The radiation patterns of the closed D_5, F_5 and F_{m5} versions at the first band frequencies 1200 MHz, 1155 MHz and 1158 MHz respectively compared with straight monopole resonant at 1900 MHz.

Chapter 5

THE EFFECT OF THE GEOMETRY ON THE FRACTAL TREE ANTENNAS

The geometry of the proposed fractal tree antennas is changed. To improve the resonance behavior of the antennas in the previous chapter, it is expected that the change in geometry affects the resonance frequency of the fractal tree antennas. Also, the number of branches is increased according to the Fibonacci number sequence. The tree, whose branches are increasing from the base to the tip of the antenna according to the Fibonacci number sequence, is called ‘Dream tree’.

5.1 Geometrical Changes on the Antennas

5.1.1 *D* version Fractal Tree Antennas

The initiator of the fractal tree antennas is a monopole. Then at the first iteration step the monopole is divided into two branches. Each branch is splitting with an angle 30° through left and right at the second iteration step. The process is applied to the remaining branches until the fifth iteration. The branch length is equal to the double of the previous branch from the tip to the base of the antenna. The branch length ratios are same with the *D* version antenna given in Chapter 4. The geometry of the branches of this version is given in Figure 5.1. The antennas are open structures.

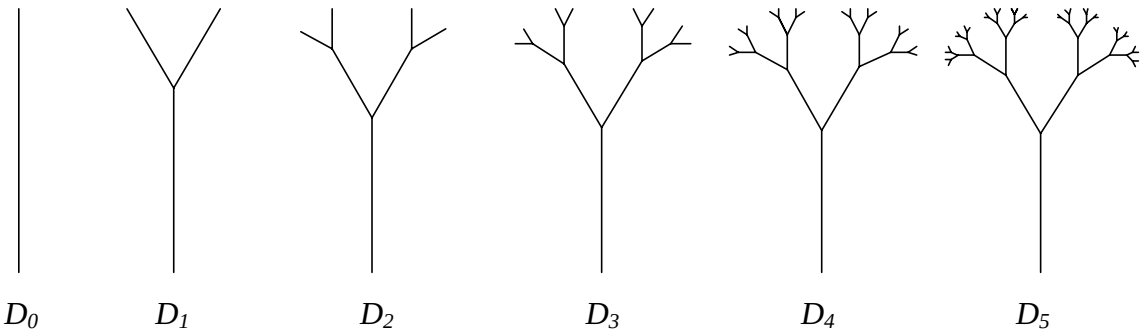

Figure 5.1 *D* version fractal tree antenna configuration with open structures.

The antenna is fed at its bottom, which is connected to an infinitely conducting plane. The length of the antennas is 3.75 cm from the base to one tip of the antenna.

Monopole antennas are divided into 60 segments from the base to one tip of the antenna. The radius of the wires is 0.0075 cm for all cases.

5.1.2 *F* version Fractal Tree Antennas

The geometry of the branches of the *F* version fractal tree antennas in Chapter 4 is modified. As shown in Figure 5.2 the branches of the trees are splitting with an angle 30° through the left and right at each iteration step. The end of the branches is getting closer while the iteration number increases. The branch lengths are increasing according to the Fibonacci number sequence and the branch length ratios are given in Chapter 4. The antennas have open structures like shown in Figure 5.2.

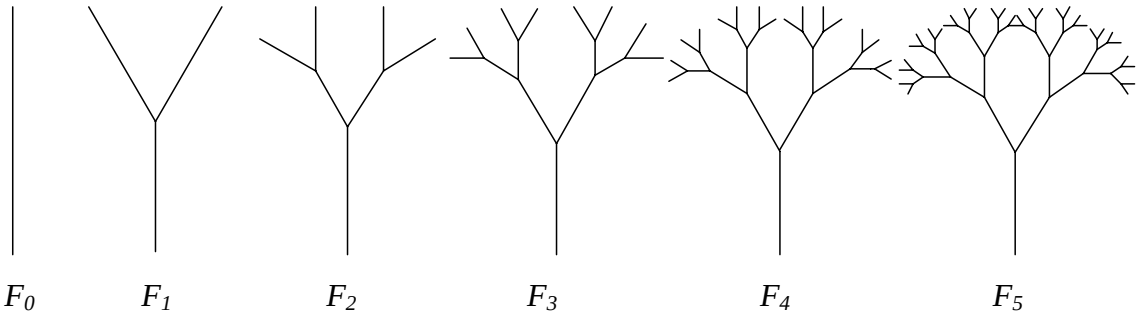

Figure 5.2 F version fractal tree antenna configurations with open structures.

The antenna is fed again at its bottom, where it is connected to an infinitely extending ground plane. The length of the antenna from the base to one tip is 3.75cm. The radius of the wires is 0.0075 cm for all cases.

5.1.3 F_m version Fractal Tree Antennas

The branch lengths and the branch length ratios are same with the F_m version in Chapter 4. The branch lengths of the trees are increasing according to the modified Fibonacci sequence. A recursive generating algorithm is applied to the monopole until the fifth iteration. Geometry of the branches are different than those of the previous F_m version antennas mentioned in Chapter 4. The branches of the fractal tree antennas are splitting with an angle 30° through the left and right. The tree configuration is shown in Figure 5.3.

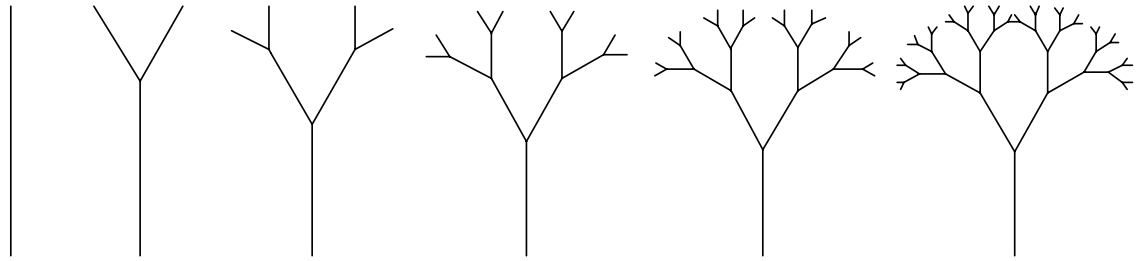

Figure 5.3 The configuration of the F_m version with open structures.

The length of the trees from the base to one tip of the last branch remains same and it is equal to 3.75 cm. Monopole antennas are divided into 60 segments. Wire radius is equal to 0.0075 cm at this time.

5.2 Dream Tree Antennas

5.2.1 *D* version Dream Tree Antennas

The tree, whose number of branches is increasing according to the Fibonacci sequence, is called 'Dream tree'. If the branch lengths of the Dream tree antenna are increasing according to the number sequence 1, 2, 4, 8, 16, 32, … then the antenna is called *D* version Dream tree. The geometry of the *D* version Dream tree antenna is given in Figure 5.4. The branch lengths and the branch length ratios of the *D* version Dream tree antenna are same with the previous *D* version fractal tree antenna in Chapter 4. The number of branches of the tree antennas is reduced in this case. The geometry of the branches is open like shown in Figure 5.4.

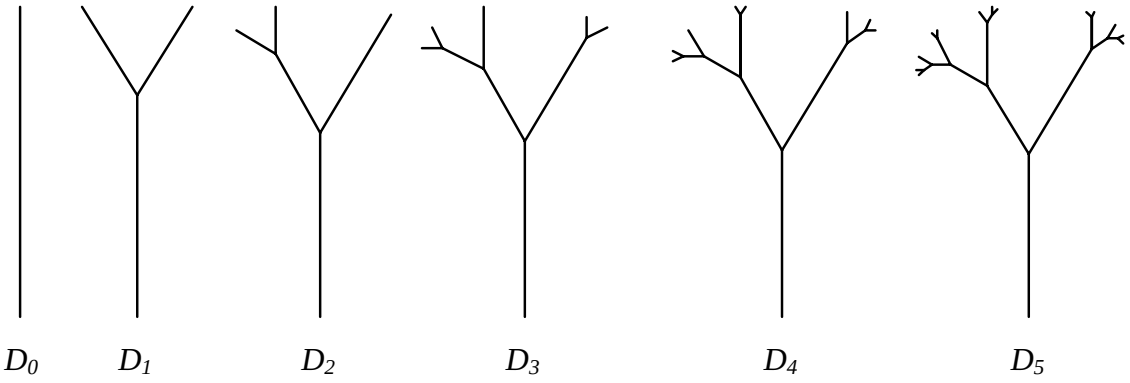

Figure 5.4 *D* version Dream Tree Antennas.

5.2.2 *F* version Dream Tree Antennas

The number of branches of the *F* version is changed according to the Fibonacci number sequence from the base to one tip of the antenna and called *F* version Dream tree. The tree configurations are shown in Figure 5.5. The change in the branch lengths and branch length ratios of this dream tree antenna are same with the *F* version. However the number of branches of dream trees is less than those of *F* version and dream tree antennas are less complex structures.

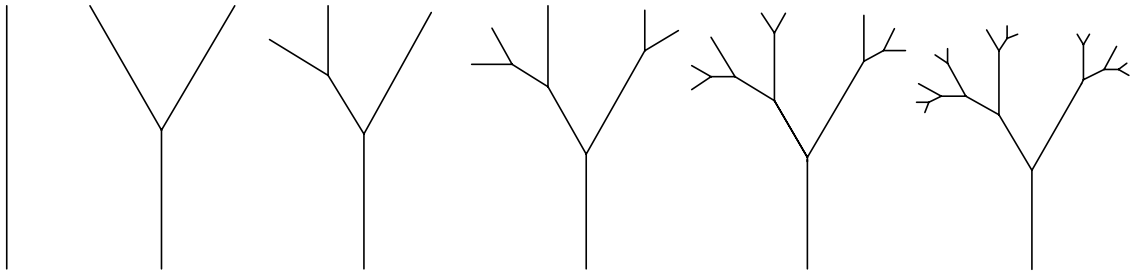

Figure 5.5 *F* version Dream tree configurations.

5.2.3 F_m version Dream Tree Antennas

The number of branches of the F_m version is changing according to the Fibonacci sequence from the base to one tip of the antenna and called F_m version dream tree. The tree configurations are shown in Figure 5.6. A recursive generating algorithm is applied to a monopole until the fifth iteration. Branch lengths and branch length ratios are same with the F_m version. The number of branches is increasing according to the Fibonacci sequence from the base to one tip of the antenna. The antenna has an asymmetric branch geometry.

The length of the antennas is same from one of the tips to the base and equal to 3.75 cm. Monopole antennas are divided into 60 segments, whose lengths are equal to 0.0625 cm. The radius of the wires is 0.0075 cm.

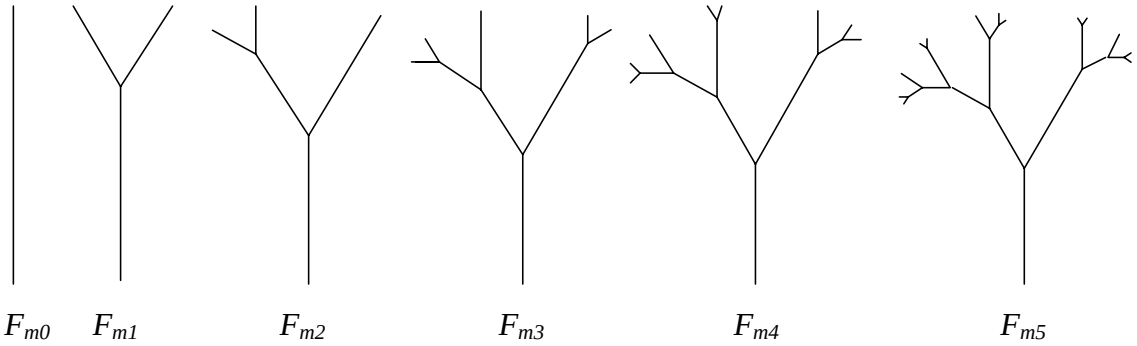

Figure 5.6 F_m version dream tree configurations.

5.3 Results

Figure 5.7 shows the input reflection coefficients of the fractal tree antennas. The resonance frequencies of the antennas are decreasing while the iteration number increases. The resonance frequencies of the antennas with same geometries are affected from the total conducting path lengths. For Dream tree antennas the total conducting path lengths are reduced, so the decrease in resonance frequency becomes less than the open *D, F* and F_m version fractal tree antennas like shown in Figure 5.7.

The 3 dB bandwidths of the open structures are nearly same, 22%. The 10 dB bandwidths of the antennas change between 5% and 6%.

The overall quality factors (*Q)* of these antennas are shown in Figure 5.8. As given in Figure 5.8, the *Q* values are decreasing and they are approaching a limiting curve for high iteration numbers.

The overall system gains of the D version and the Fibonacci fractal tree antennas are decreasing while the iteration number increases. The antennas have maximum system gains at their resonance frequencies. As shown in Figure 5.9 the antennas have similar system gains.

The far field patterns are same with the straight dipole antenna like shown in Figure 5.10. The antennas are omnidirectional. The radiation patterns of the antennas at the first band frequencies don’t be affected from the branch length ratios and the asymmetrical tree configurations. The antennas are linearly polarized.

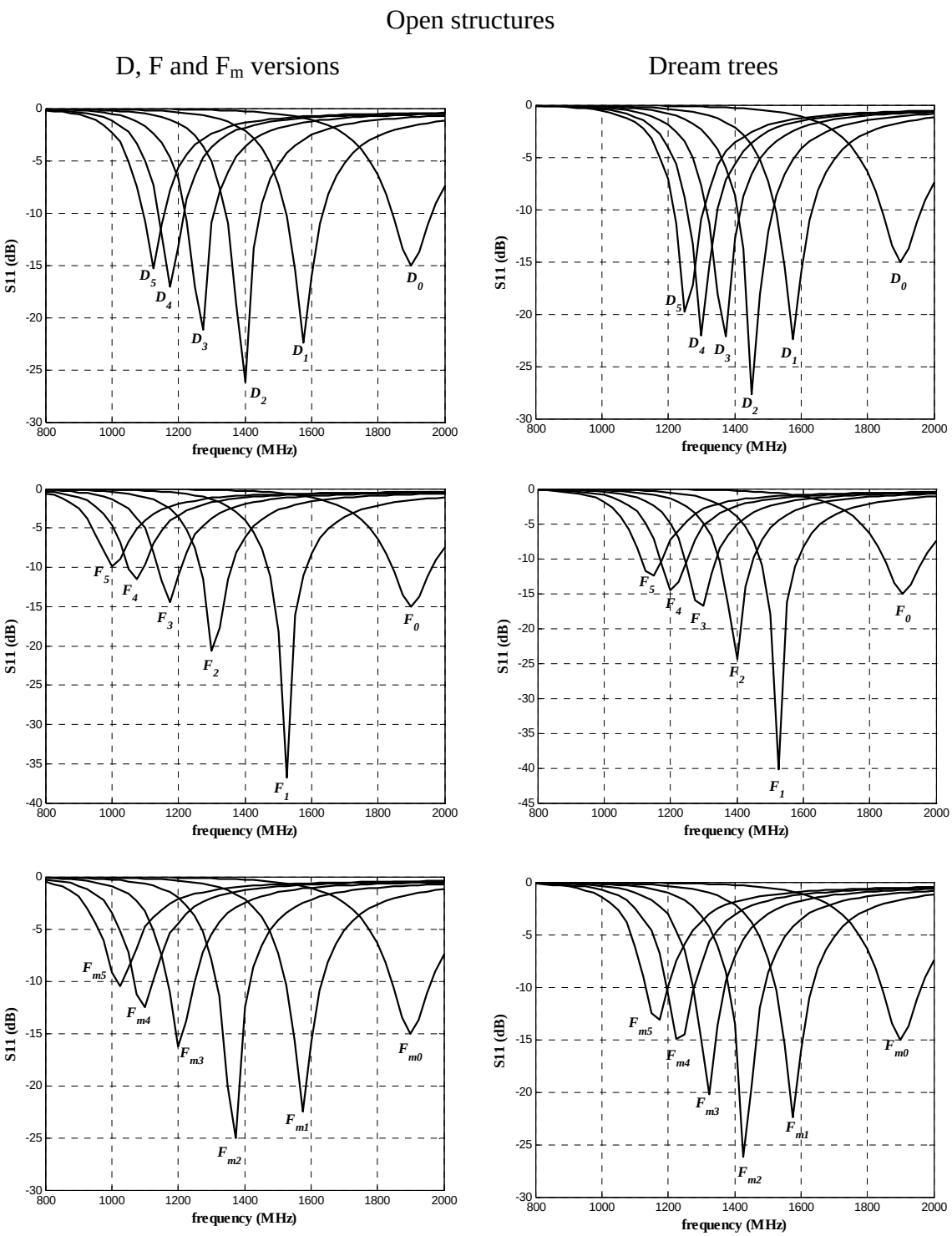

Figure 5.7 The input reflection coefficients of the *D*,*F* and F_m versions with open structures.

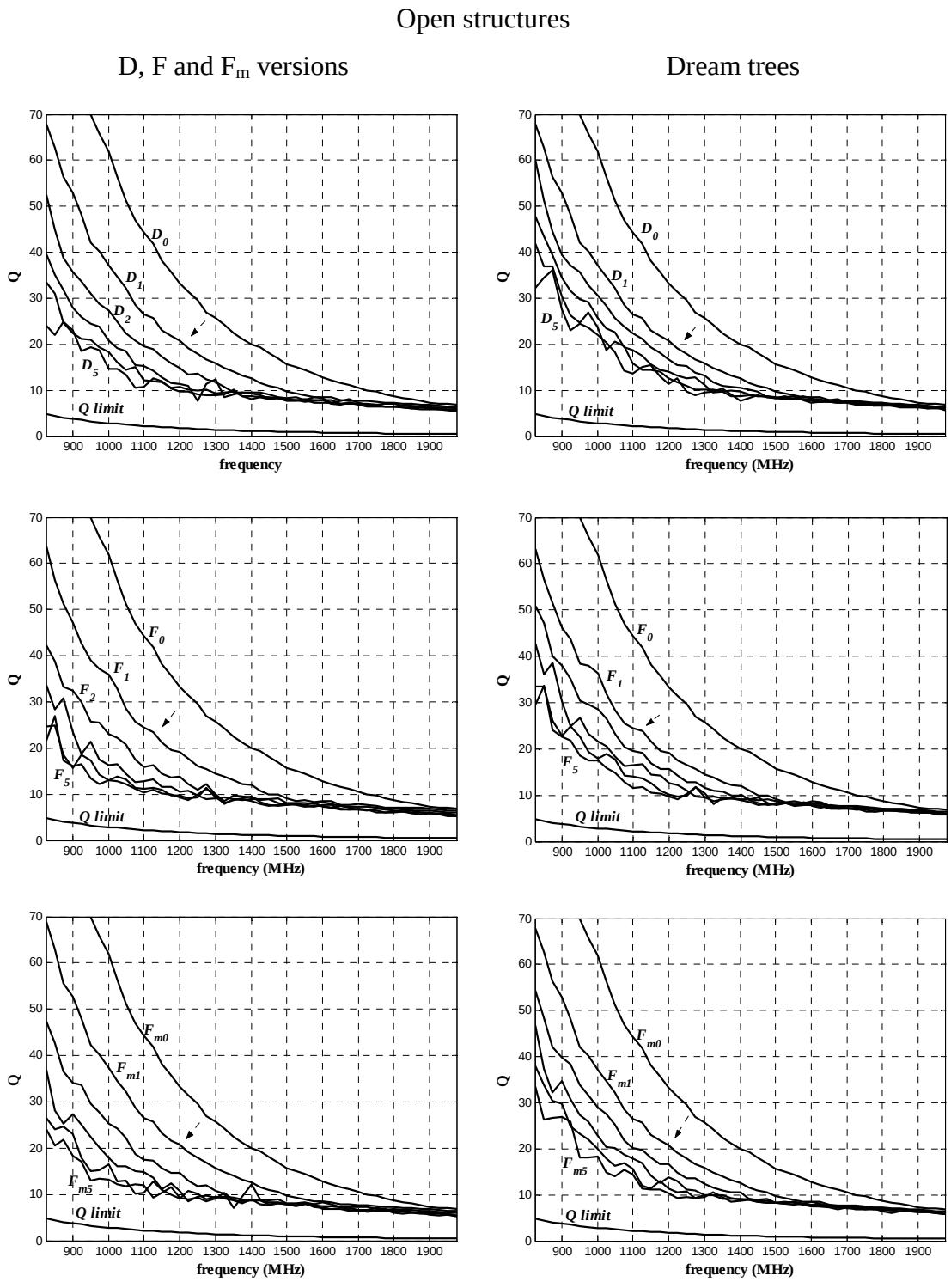

Figure 5.8 The overall quality factors of the D, F and Fm versions with open structures.

Open structures

D, F and F_m versions

Dream trees

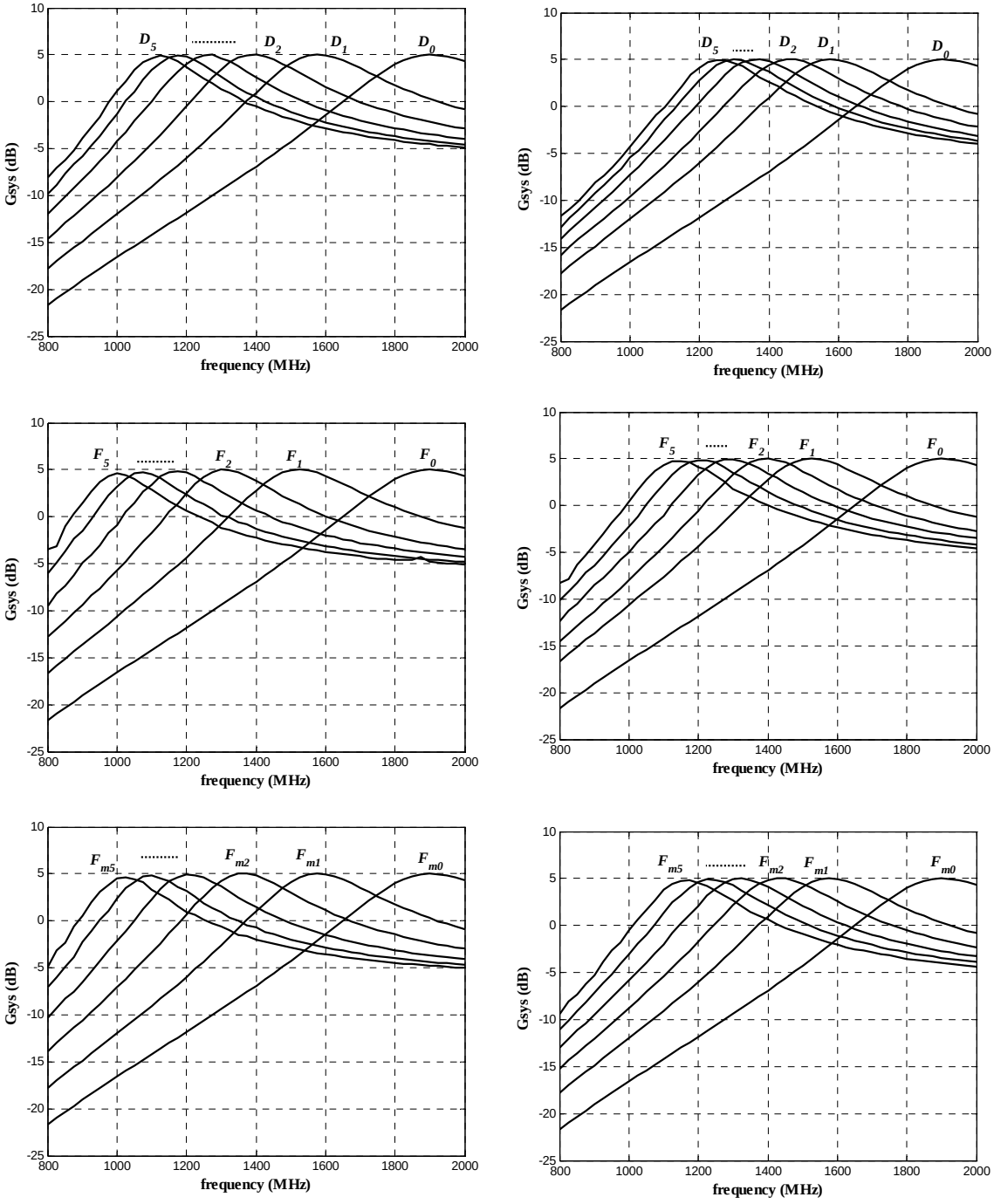

Figure 5.9 The overall system gains of the fractal tree antennas with open structures.

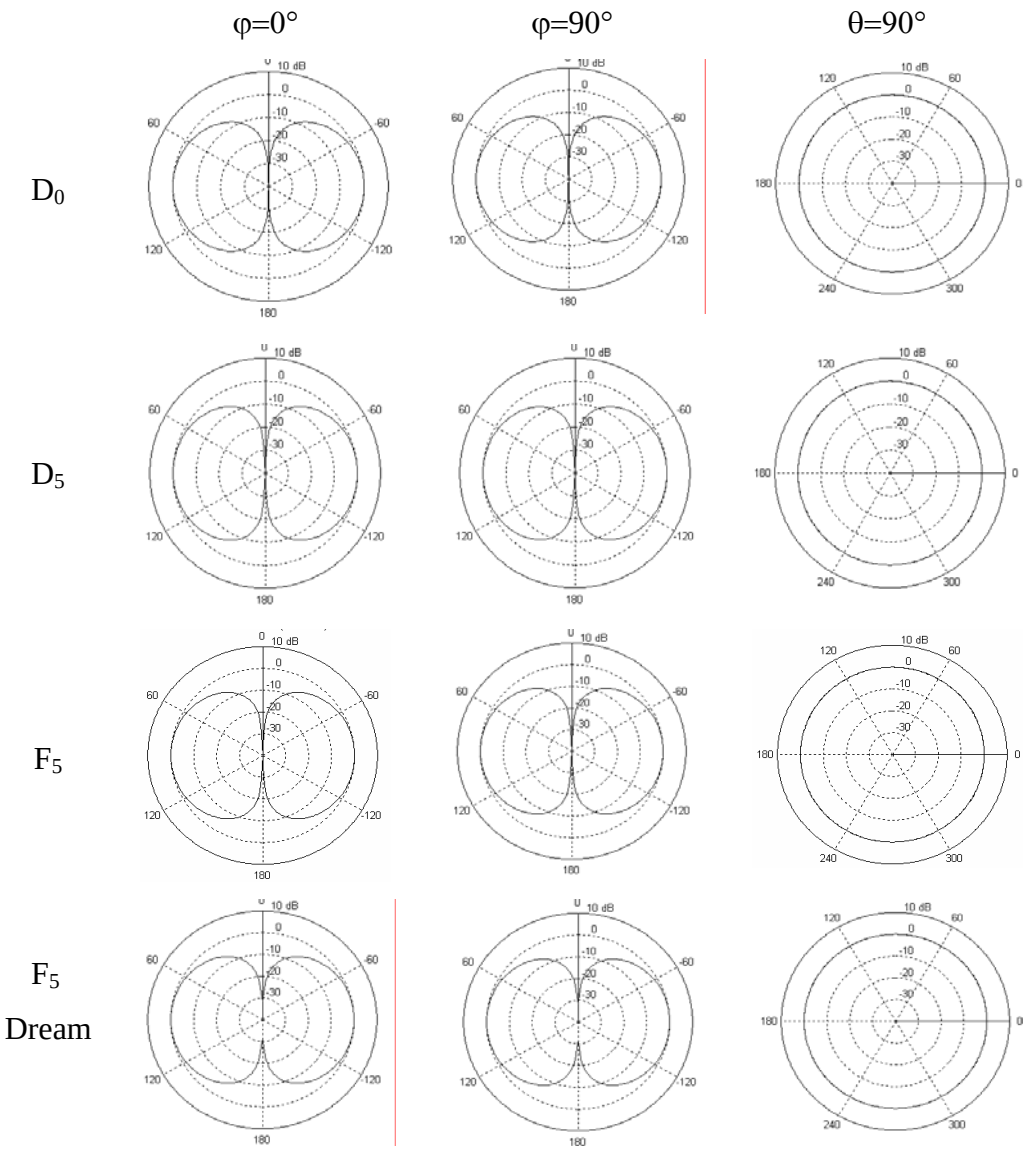

Figure 5.10 The far field patterns of the D_0, D_5, F_5 and Dream tree F_5 version antennas at the first band frequencies 1900 MHz, 1125MHz, 1000MHz and 1125 MHz respectively.

Chapter 6
COMPARISONS AND DISCUSSIONS ON THE FRACTAL TREE ANTENNAS

The results of the fractal tree antennas with closed structures are compared with the antennas with open structures. The performance of the antennas is evaluated in terms of the resonance behavior of the fractal tree antennas.

6.1 The Resonance Frequencies and the Percent Shifts

The resonance frequencies of the fractal tree antennas with different geometries are compared each other and the values are given in Figure 6.1. By examining the Figure 6.1, one can see that closed *F* version antennas are decreasing the resonance more than the closed *D* version fractal tree antennas. Furthermore, when the geometry of the branches changes and branches construct open structures, the performance of the antennas in decreasing resonance frequency is improved.

The resonance frequencies and the percent shifts of the fractal tree antennas with closed structures are compared with those of the open structure in Table 6.1. As shown in Table 6.1, closed *F* is better than the closed *D* version in decreasing resonance frequency. However, open structures have lower resonance frequencies than the closed structures. Furthermore, same performance can be get at lower iterations by using Fibonacci antennas, which are similar but simpler structures compared to *D* version. The miniaturization effect of the *F* versions is more than that of the *D* version. The percent resonance frequency shifts of the closed *F* and F_m versions with respect to the *D* version are decreasing while the iteration number increases. They are closing each other at high iteration levels. On the other hand, the percent resonance frequency shifts of the open antennas are increasing while the iteration number increases. It can be said that open *F* and open F_m are better in decreasing resonance frequency than their closed structures.

The resonance frequencies of the closed antennas are compared with those of the open antennas in Figure 6.2. For closed antennas, the resonance frequencies of the *F* and F_m versions are close to each other while the iteration number increases. The Fibonacci antennas are better than the *Double* version in decreasing resonance frequency. Open structures have lower resonance frequencies than the closed structures.

Additionally, lowering the resonance frequency has the same effect as miniaturizing the antenna at a fixed resonant frequency. Generally, the miniaturization effect of the Fibonacci antennas are more than the *Double* version fractal tree antennas.

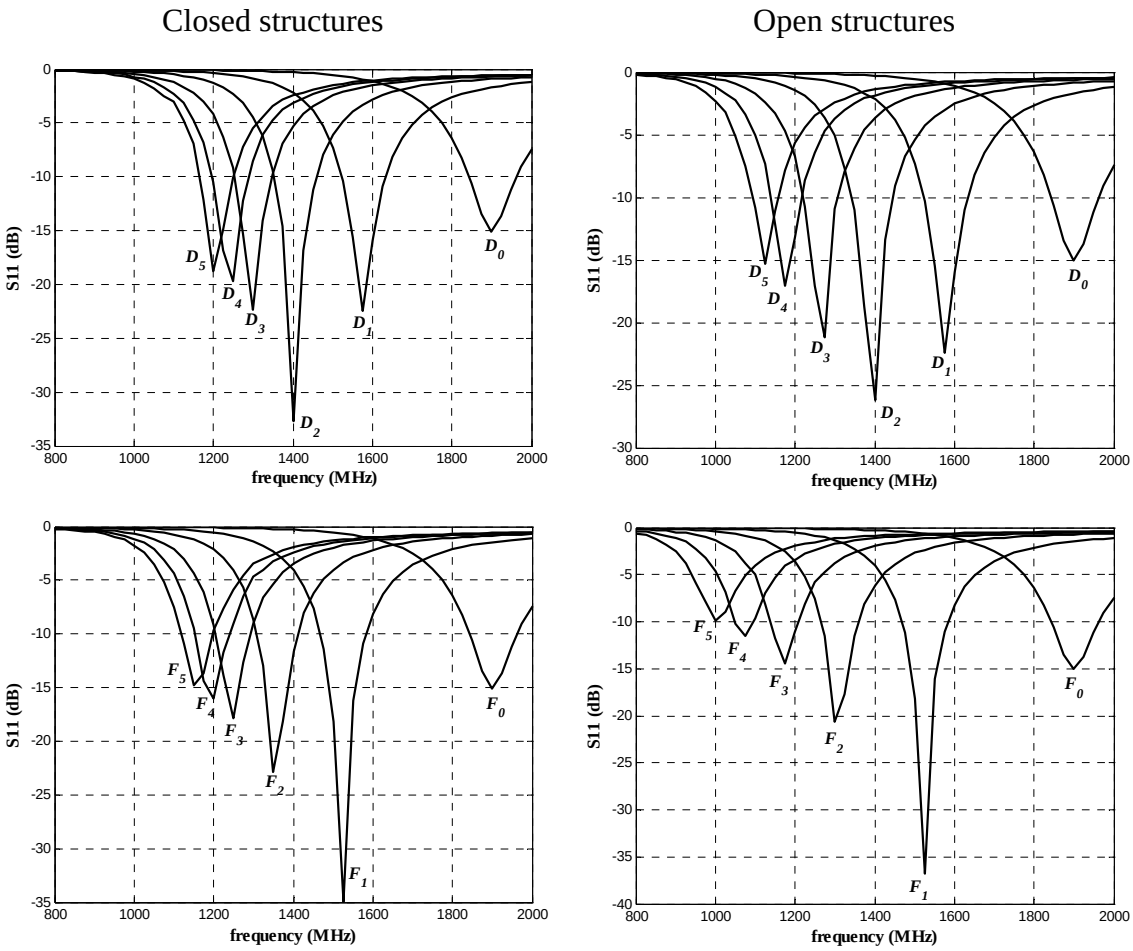

Figure 6.1 The comparison of the input reflection coefficients of the *D*, *F* and F_m version fractal tree antennas.

Table 6.1 The resonance frequencies* and the percent shifts shifts.

	Closed structures					Open structures				
itr	$f_{res,D}$	$f_{res,Fm}$	% Shift	$f_{res,F}$	% Shift	$f_{res,D}$	$f_{res,Fm}$	% Shift	$f_{res,F}$	% Shift
0	1900	1900	-	1900	-	1900	1900	-	1900	-
1	1590	1590	-	1550	13	1590	1590	-	1550	12.9
2	1400	1360	8	1350	10	1392	1351	8	1308	16.5
3	1300	1255	7.5	1250	8.3	1262	1207	8.6	1168	14.7
4	1245	1200	6.8	1195	7.6	1174	1090	11.5	1065	15
5	1200	1158	6	1155	6.4	1125	1019	13.6	1000	16.1

*Resonance frequencies are given in MHz.

Closed structures Open structures

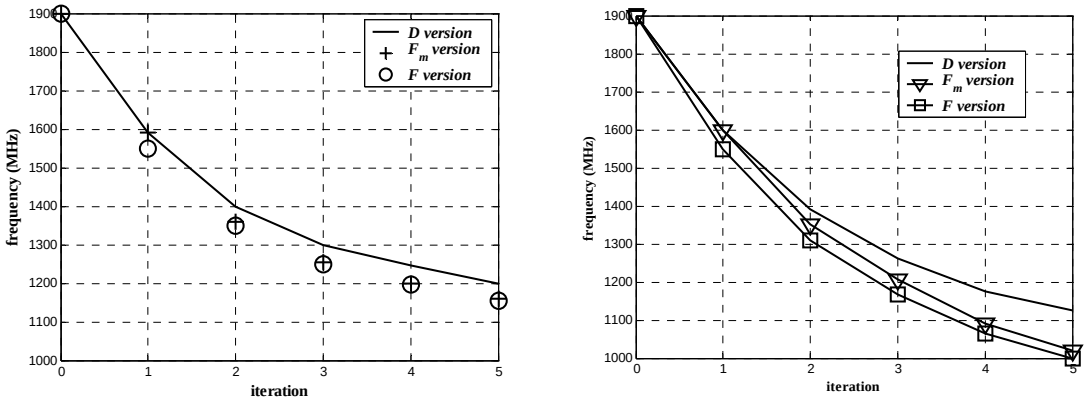

Figure 6.2 The relative comparison of the resonance frequencies of the closed and open fractal tree antennas**.**

Open *D* version is compared with the closed *F* version and *F* version Dream tree antennas in Table 6.2. Closed *F* has similar miniaturization effect on the antennas with *D* version even though its geometry is different than the *D* version. Same performance can be get by using *F* version Dream tree, which are similar structures compared to *D* version.

Table 6.2 The comparison of the resonance frequencies* of the open *D* version with the closed *F* and Dream tree *F* version antennas.

itr	*D* version with open structures	*F* version with closed structures	*F* version Dream tree
0	1900	1900	1900
1	1590	1550	1550
2	1392	1350	1400
3	1262	1250	1275
4	1174	1195	1200
5	1125	1155	1125

* Resonance frequencies of the antennas are given in MHz.

The resonance frequencies of the open *D* version, closed *F* version and *F* version Dream tree antennas are given in Figure 6.3. These structures have same miniaturization effects on the antennas at a fixed resonance frequency.

The resonance frequencies of the *F* version Dream tree antenna are similar with the *D* version. The *F* version Dream tree antennas are less complex than the *D* version. So, same performance can be obtained with using simple fractal structure instead of complex one.

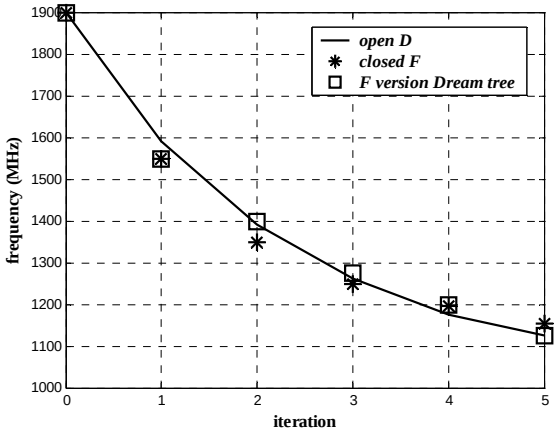

Figure 6.3 The relative comparison of the resonance frequencies of the open *D*, closed *F* and Dream tree *F* version antennas.

6.2 The Quality Factors at Resonance Frequencies

The overall quality factors of the fractal tree antennas are decreasing while the iteration number increases. However the quality factors of the fractal tree antennas at resonance frequencies are increasing while the iteration number increases. In Figure 6.4 the quality factor of the D_5 and F_5. and F_{m5} versions at the resonance frequencies are given. The quality factors for closed structures in Figure 6.4 change between 7 and 10, while for open structures they change between 7 and 13 and 7 and 12. However, the difference between the *Q* values at resonance frequencies is smaller than the difference between resonance frequencies of the antennas. For example the difference between the *Q* values of open F_5 and open F_4 antennas is 1.75 while the difference between resonance frequencies is 65 MHz.

The fractal dimensions are increasing while the iteration number increases. When the geometry of the branches changed, the fractal dimension of the antennas didn't change noticeably.

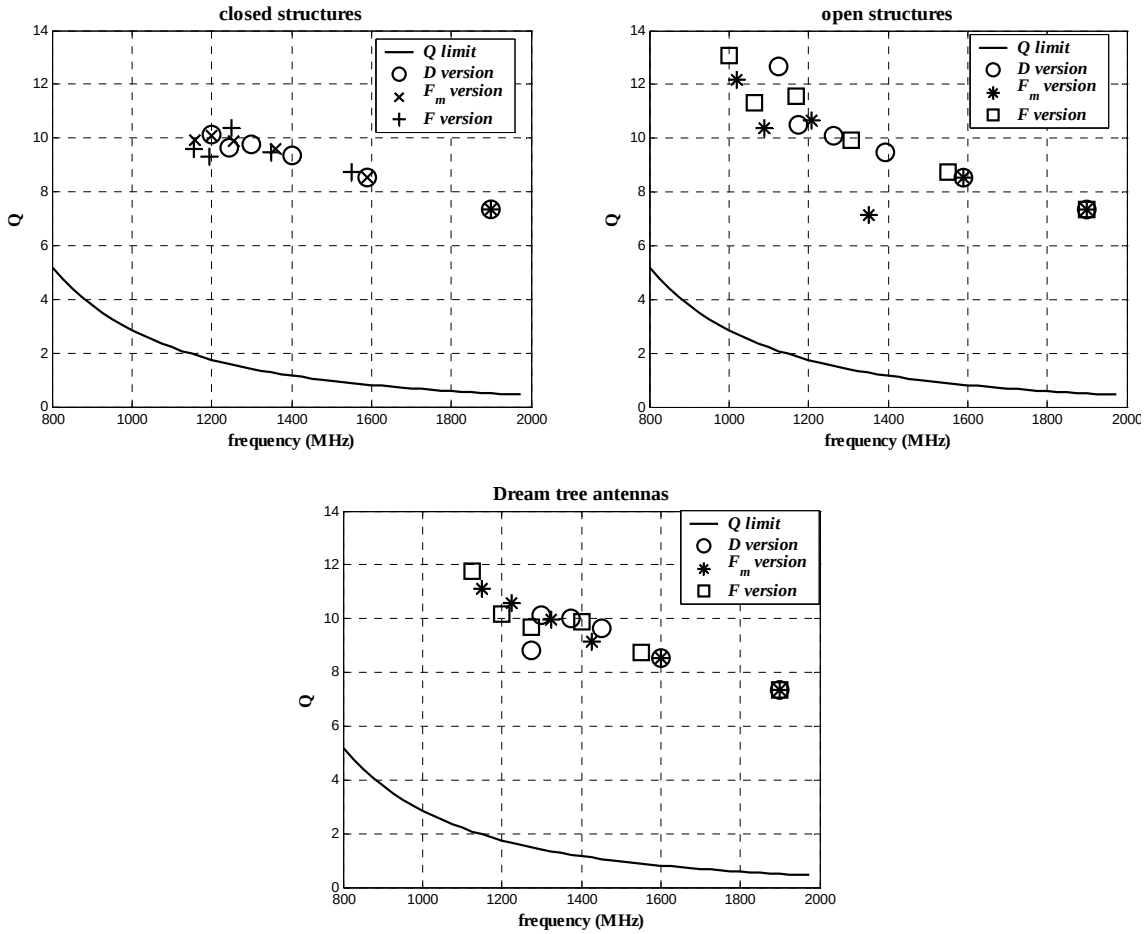

Figure 6.4 The quality factors at resonance frequencies of the fractal tree antennas.

Chapter 7

MULTIBAND BEHAVIOR OF THE FRACTAL TREE ANTENNAS

There is a relation between the properties of fractal geometry and electromagnetic behavior of an antenna. Fractal geometry has self-similar forms, which can lead to multiband characteristics in antennas that is displayed when an antenna operates with a similar performance at various frequencies. Sierpinski antenna is given as an example for a multiband antenna.

In this chapter the multiband properties of the fifth iterations of *D* version, *F* version and the *F* version Dream tree are investigated. There are two reasons to choose these three antennas for simulations. One of them is that the antennas have nonuniform branch length ratios and similar forms. It is investigated whether they have multiband property or not like Sierpinski antenna, which has self-similar form and uniform scale factor. The other reason is about Dream tree antennas. Dream tree antennas have asymmetric branch geometry. It is investigated that the asymmetry of the fractal trees are affecting the multiband behavior or not.

7.1 D_5 version Fractal Tree Dipole Antenna

The multiband behavior of the D_5 version is observed. The tree configuration is shown in Figure 7.1. The antenna in Figure 7.1 is the fifth iteration of the *D* version fractal tree antenna, whose branches are splitting with an angle 30° through left and right. The branch lengths of the antennas are the double of the previous branches and the branch lengths are increasing according to the number sequence 1, 2, 4, 8, 16, 32, 64,… from the tip of the antenna to the center of the dipole. So they have uniform branch length ratios.

The antenna is fed at its center. The antenna is 7.5 cm from one of the tips of the antenna to the other tip. The radius of the wires is 0.0075 cm and 120 segments are used from one tip of the antenna to the other tip.

The resonance frequencies for five bands are given in Figure 7.2. The antenna shows same performance at various frequencies. It can be said that the multiband behavior is consistent from the input return loss.

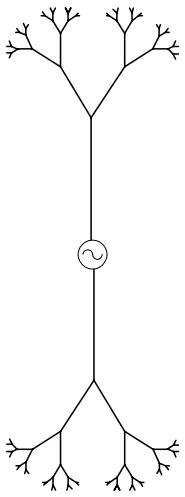

Figure 7.1 D_5 version fractal tree dipole antenna.

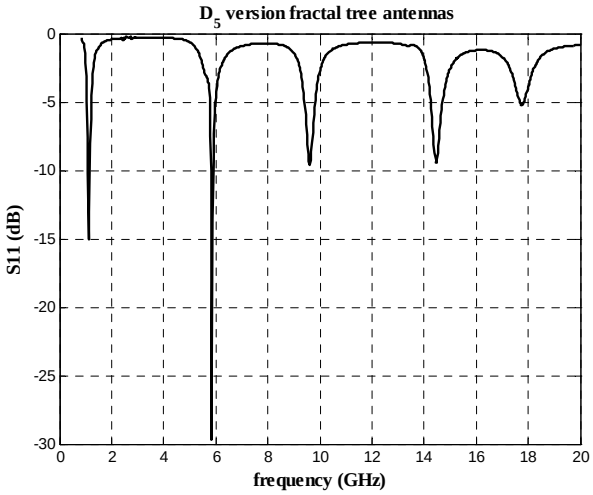

Figure 7.2 The input reflection coefficients of the D_5 version fractal tree dipole antenna.

Five frequency bands of the D_5 version are investigated in Table 7.1. The frequencies (f_n) are given in the second column. The relative bandwidth at each band for VSWR<2 is nearly 6.6%. The third one is the input return loss (S11) and the fourth one represents the frequency ratio between two adjacent bands. The antenna has similar performance at various frequencies, so it shows multiband behavior.

Table 7.1 The parameters of the D_5 version antenna for the five band frequencies.

n (band n°)	f_n (MHz)	S11 (dB)	f_{n+1}/f_n
1	1125	15.1	5.22
2	5875	29.1	1.63
3	9625	9.59	1.5
4	14500	9.39	1.22
5	17775	5.23	-

The far field patterns of the D_5 version dipole antenna at the first frequency band is given in the previous chapter. The patterns of the first frequency band are compared with the second, third, fourth and fifth frequency bands in Figure 7.3. The simulated antennas are placed in the x-z plane. While the frequencies are increases the variations on the side lobes are faster. The omnidirectional behavior of the antennas is disturbing after the second frequency band. It can be said that the elevation patterns (φ=0°, and φ=90°) are approximately similar at the band frequencies.

7.2 F_5 version Fractal Tree Dipole Antenna

The fifth iteration of the *F* version fractal tree antenna is given in Figure 7.4. The branch lengths of the trees are increasing according to the Fibonacci sequence 1, 1, 2, 3, 5, 8, … from one of the tips to the center of the dipole. F_5 version has nonuniform branch length ratios.

The length from one of the tips to the other tip of the F_5 version antenna is 7.5 cm. The radius of the wires is 0.0075 cm and the segment length is *l* (length of the antenna)/120, which nearly equals to 0.0625 cm. The feed is located at the center of the antenna.

The resonance frequencies for five bands are given in Figure 7.5. The antenna has same performance at various frequencies. It behaves like a multiband antenna.

Five band frequencies are investigated for the F_5 version in Table 7.2. The relative bandwidth at each band for VSWR<2 is nearly 4.5%. The ratios between two adjacent bands of the F_5 version are closer to those of the D_5 version, even though the branch lengths and branch length ratios are different than D_5.

The far field patterns of the five bands are given in Figure 7.6. The ripples on the far field patterns are increasing after the first band frequency. The omnidirectional behavior is disturbing while the band frequency is increasing. The elevation patterns of the F_5 version are approximately similar.

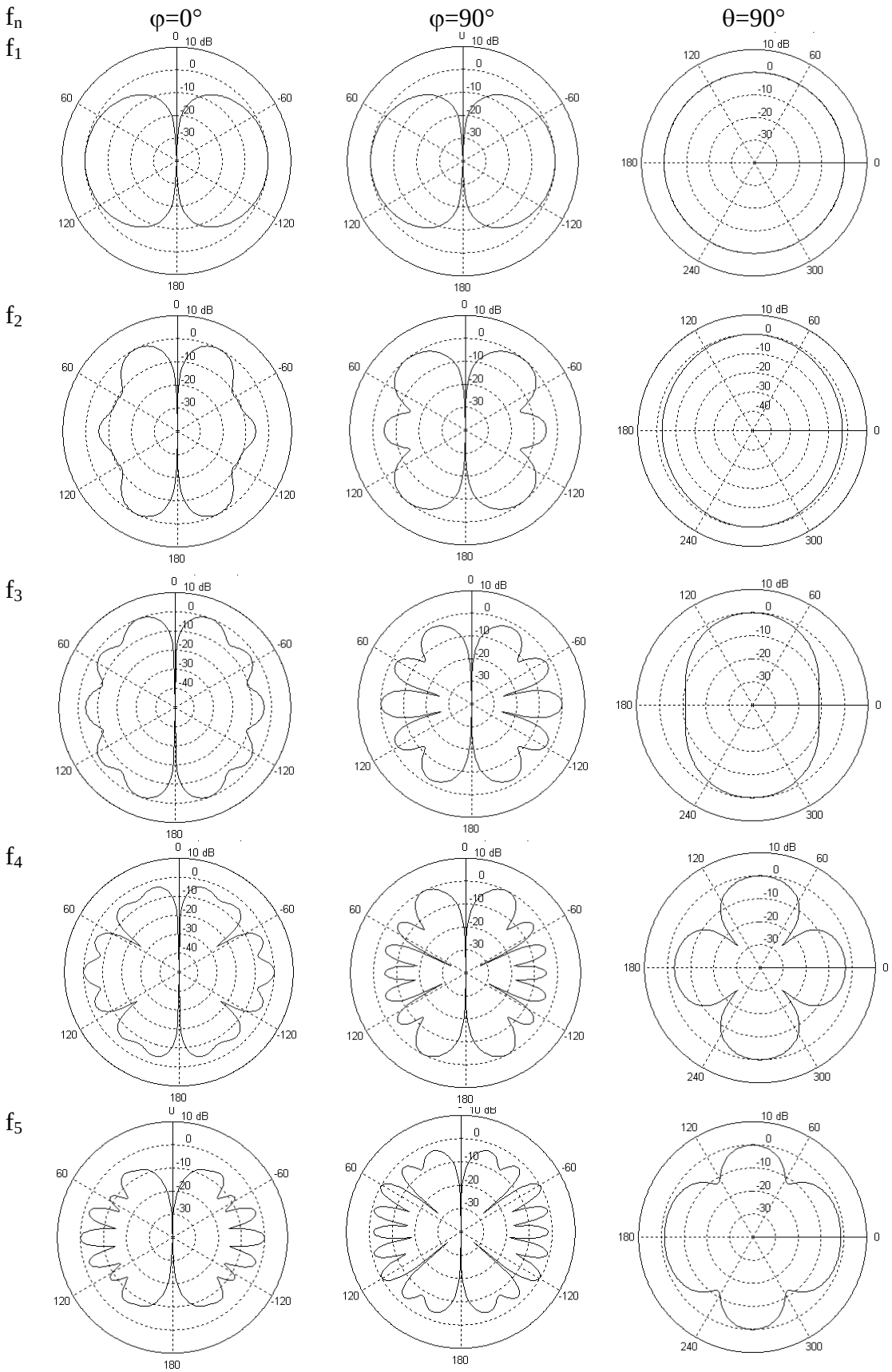

Figure 7.3 The radiation patterns of D_5 version for the band frequencies f_1-f_5.

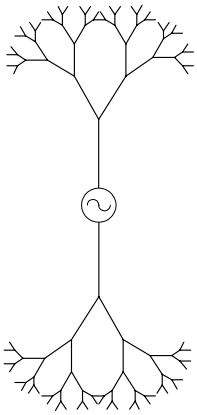

Figure 7.4 F_5 version fractal tree dipole antenna.

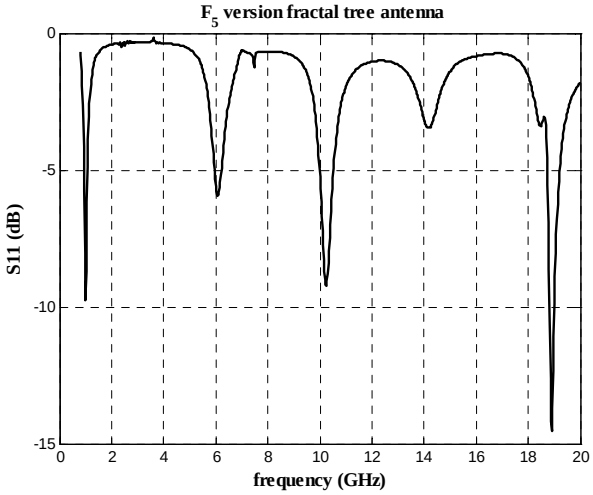

Figure 7.5 The input reflection coefficients of the F_5 version fractal tree dipole antenna.

Table 7.2 The parameters of the F_5 version antenna for the five band frequencies.

n (band n°)	f_n (MHz)	S11 (dB)	f_{n+1}/f_n
1	1000	9.8	6.05
2	6050	5.92	1.69
3	10250	9.21	1.38
4	14150	3.48	1.33
5	18875	14	-

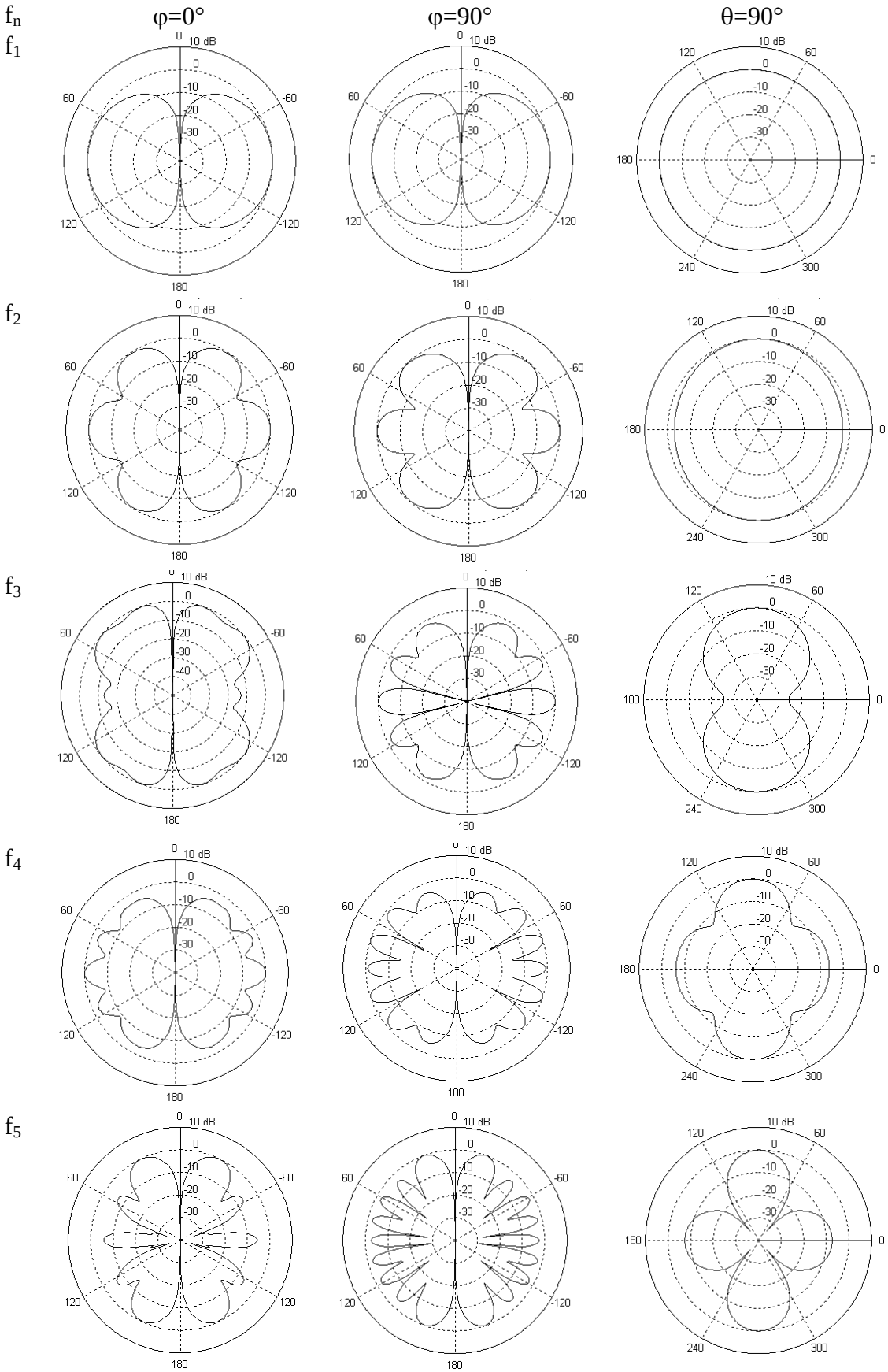

Figure 7.6 The far field patterns of the f_1-f_5 band frequencies of the F_5 version.

7.3 F_5 version Dream Tree Dipole Antenna

The fifth iteration of the *F* version dream tree is given in Figure 7.7. The number of branches are increasing according to the Fibonacci sequence, which corresponds to a sequence 1, 1, 2, 3, 5, 8,… from the center to the one of the tips of the dipole. The branch lengths are increasing again according to this special sequence from one tip of the antenna to the center.

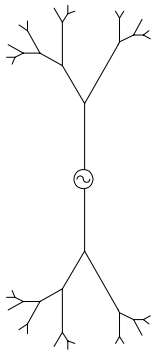

Figure 7.7 The configuration of the F_5 version dream tree dipole antenna.

The length is 7.5 cm from one of the tips to the other tip. The radius of the wires is 0.0075 cm. Segment lengths of the antennas are equal 0.0625 cm.. The antenna is fed at its center.

The five band frequencies are given in Figure 7.8. By examining the Figure 7.8, one can see that F_5 version Dream tree has similar performance at various frequencies.

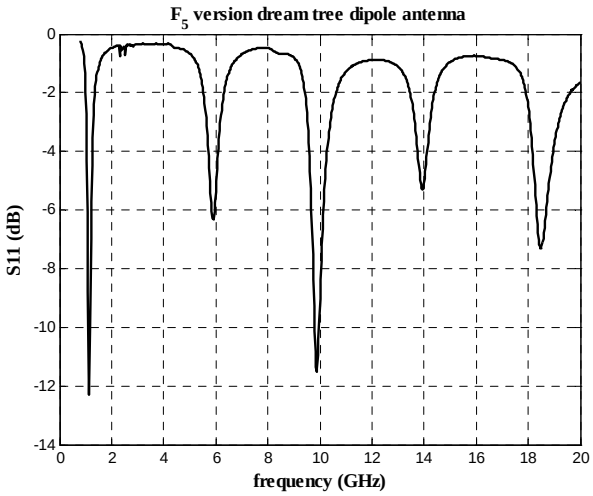

Figure 7.8 The band frequencies of the F_5 version dream tree dipole antenna.

The five frequency bands are given in Table 7.3. The bandwidth at each band is nearly 5.7%. The ratios of two adjacent bands of F_5 version dream tree antenna is nearly equal to D_5 version, even though they have less number of branches and nonuniform branch length ratios compared to *D* version.

Table 7.3 The parameters of the F_5 version Dream antenna for the five band frequency.

n (band n°)	f_n (GHz)	S11 (dB)	f_{n+1}/f_n
1	1125	11.9	5.28
2	5950	6.05	1.65
3	9850	11.3	1.41
4	13950	5.32	1.32
5	18425	7.14	-

The far field patterns for five frequency bands are given in Figure 7.9. The ripples are increasing while the band frequencies are increasing. The effect of the asymmetry of the branch geometry occurs after the second band frequency while φ=0°. The omnidirectional property is disturbing after the first frequency band. The elevation patterns of the *F* version Dream tree antennas are approximately similar.

7.4 Comparison of the Multiband Behavior of the D_5, F_5 and F_5 version Dream Tree

The length of the antennas compared in this chapter is 7.5 cm from one tip to the other tip of the antenna. There is a relation between electromagnetic behavior and the geometrical properties of the antennas. Because of the similarity, the fractal tree antennas are behaving like multiband antennas. The return losses of the compared antennas are given in Figure 7.10. They have similar performance at various frequencies. The frequency ratios between two adjacent bands are nearly similar each other. The multiband behaviour is consistent from the input return losses of the antennas.

The radiation patterns for the first band are equal to the straight dipole. As a comparison the radiation patterns for the second band frequency is given in Figure 7.11. All antennas show similar performance at the second band frequencies. The elevation patterns of the F_5 and Dream tree F_5 are same. All antennas have same directionality at the second band frequency.

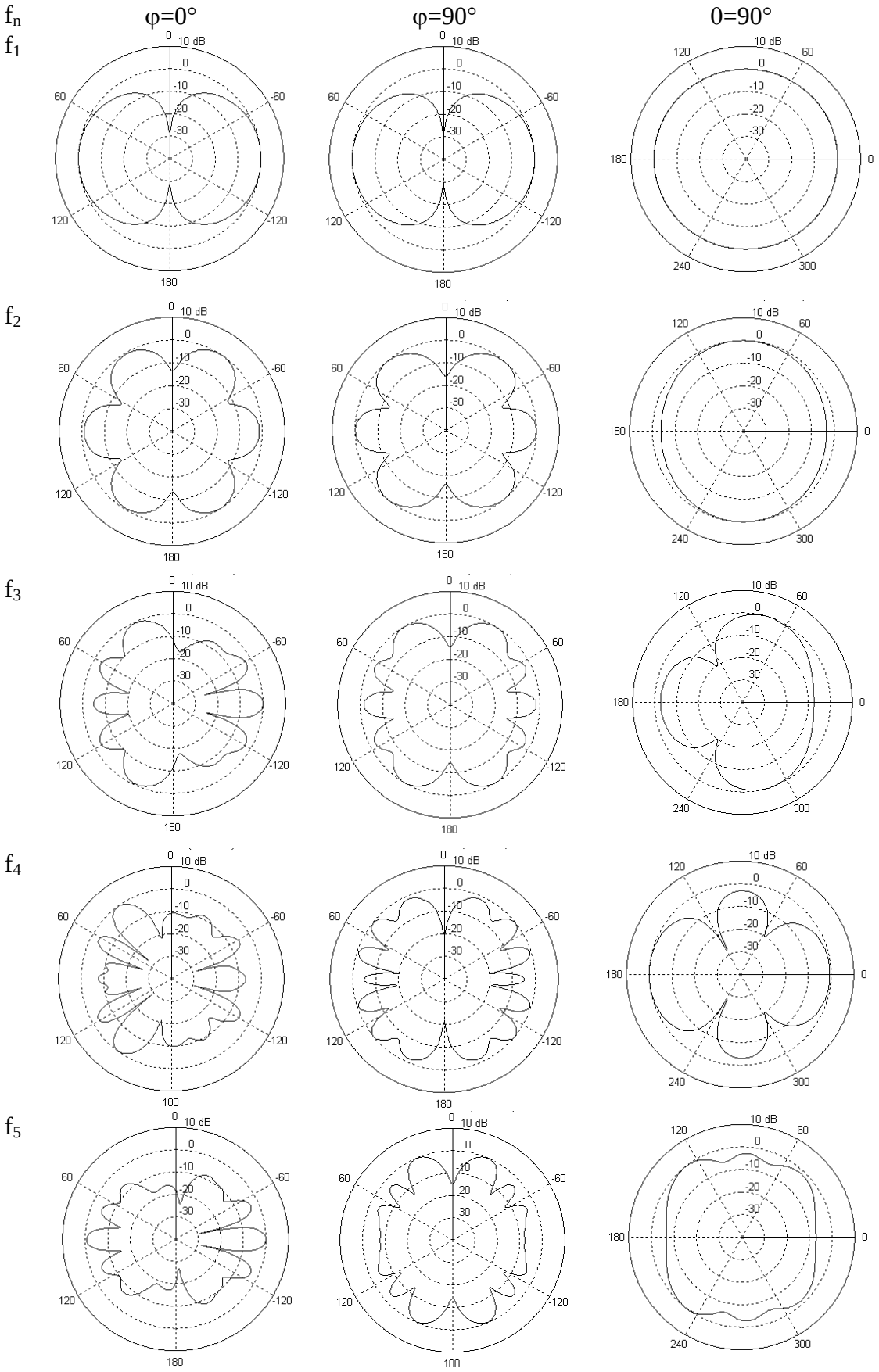

Figure 7.9 The far field patterns of the f_1-f_5 band frequencies of *F_5* version dream tree.

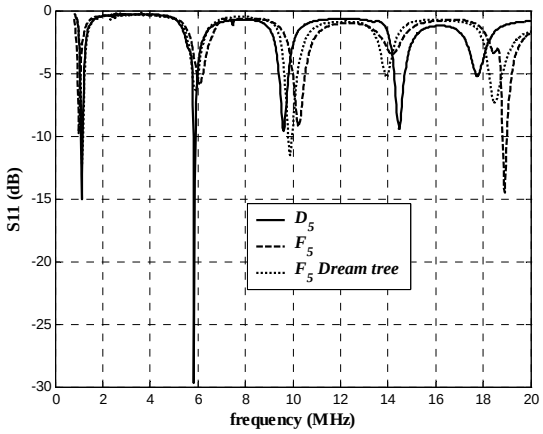

Figure 7.10 The five band frequencies of the D_5, F_5 and and dream tree F_5 version.

Elevation pattern
φ=0°, 0°≤θ≤180°.

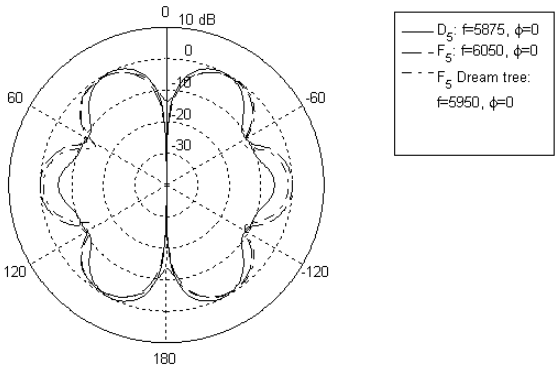

Azimuth pattern
θ=90°, 0°≤φ≤360°.

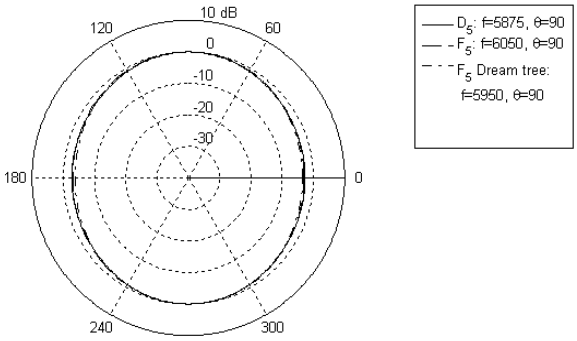

Elevation pattern
φ=90°, 0°≤θ≤180°.

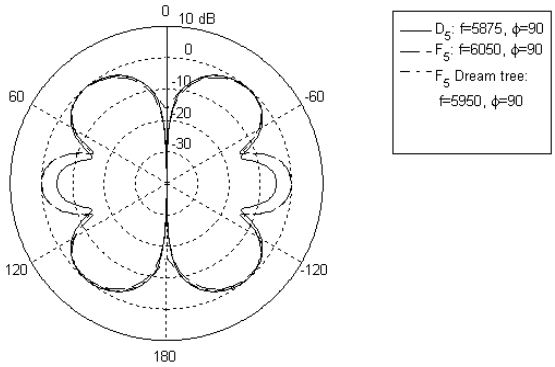

Figure 7.11 The radiation patterns of the second band frequencies of D_5, F_5 and Dream tree F_5 version antennas.

Chapter 8

APPLICATIONS OF THE FRACTAL ANTENNAS

Many fractal antennas are used in communication systems. The sudden increase in wireless communication systems causes a need for small and efficient antennas. Wireless communication systems have attracted a great amount of interest in recent years. The advances in cellular systems, wireless Local Area Networks (LANs), personal area networks, and sensor networks are bound to play a significant role in the way people will communicate with each other in the future. It is expected that in the following years most of the access part of the internet will be wireless, and wired networks will retreat to the backbone and core segments of the network.

In wireless communication systems, the antenna is the interface between the electronics of the terminal and the wireless medium. The specifications of this interface and its performance play a significant role in the acceptability of a wireless communications product. Characteristics like aesthetics, endurance, size, cost, and signal quality of a product are greatly affected by its antenna design. Therefore, the understanding of antenna capabilities and specifications is essential in order to be able to evaluate and choose the best antenna for a certain application.

Fractal antennas can enhance radiation of electromagnetic energy from electric systems. Fractal antennas have therefore the potential to be efficient. For example, a monopole based on the Koch fractal curve is more efficient than an ordinary monopole of same size. Fractal configurations can decrease the resonance frequencies of the standard monopole antennas. Hence lower resonance frequencies cause a miniaturization effect on the antennas. Fractal structures with a self-similar geometric shape consisting of multiple copies of themselves on many different scales have multiband behaviour. Because of these special properties of the fractal antennas they are used in many wireless communication areas. Motorola has started using fractal antennas in many of its cellular phones, and reports that they're 25% more efficient than the traditional piece of wire [37]. They're also cheaper to manufacture, can operate on multiple bands, and can be put into the body of the phone. Additionally, Fractenna is the company which sells the fractal antennas. The benefits depend on the fractal applied, frequency of interest, and so on [38].

Fractal antennas can also decrease the area of a resonant antenna, which could lower the radar cross section (RCS). This benefit can be used in military applications where the RCS of the antenna is an important parameter.

In the Electrical Engineering department of the University of California many fractal antennas are designed and many applications are made in the laboratories to miniaturize the standard monopole antennas [39].

Chapter 9

CONCLUSION

Fractal geometry is used to define irregular sets. Its dimension isn't an integer. In nature many complex shapes can be found, which can be defined with fractal geometry, such as clouds, mountains, coastlines and snowflakes. You can define many problems with fractal geometry, which you can't understand and solve with Euclidean geometry. Fractal geometries have many distinct properties, which separated them from Euclidean one.

So far many self-similar fractal structures have been used in antenna designs. Sierpinski, Koch curve and Minkowski loop are examples to self-similar fractal structures, which are mostly used in many applications. The electromagnetic behavior of the antennas related with the properties of the fractal geometry. Sierpinski antennas behave like a multiband antenna because of their self similarity. They have similar performance at various frequencies. Koch and Minkowski loops are efficient and small antennas. Longer antennas can be packed in a given small volumes when using these fractal loops instead of Euclidean loops.

Fractal tree configurations are similar structures. They can be used in antenna designs to decrease the resonance frequencies of the dipoles or monopoles. So far many fractal tree antennas designed with constant branch ratios and various scale factors. In this study, the branch lengths have been changed in order to improve the performance of the antennas in decreasing resonance frequency. Fibonacci number sequence is used to design fractal tree antennas with nonuniform branch length ratios. The fractal tree antennas, which are formed by Fibonacci sequence, are better in decreasing resonance frequency than Double (D) version. Same performance can be get at lower iterations by using Fibonacci version fractal tree antennas, which are similar but simpler structures when compared to the Double version. Because the tree structures were similar each other the same quality factors and overall system gains obtained at the end of the simulations. The far field patterns of the fractal tree antennas were same with straight monopole antenna at first resonance frequencies. Their radiation patterns were omnidirectional at the first resonance frequency.

The geometry and the number of branches of the fractal tree antennas have been changed to improve the resonance characteristic of the antenna. The geometry was an

important factor which affects the resonance frequency of the antenna. The resonance frequency decreased with changing the geometry of the branches of the trees. Lowering resonance frequency means that the miniaturization effect of the antennas increases at a fixed resonance frequency. The Fibonacci fractal tree antennas are decreasing the resonance frequencies of the standard monopole antennas without disturbing the radiation patterns of the antennas at the first band frequency. The change in geometry really affected the resonance frequencies of the antennas. The total conducting path lengths and also the fractal dimension increased while the iteration number increased. However they aren't the main reasons, which decrease the resonance frequency of the antenna.

The number of branches of the 2D fractal tree antennas was reduced in order to have same performance with a simpler fractal structure compared to Double version. Dream tree antennas' branches are increasing according to the special Fibonacci sequence. Fibonacci version dream tree antenna has same performance with the Double version, whose structure is more complex than the dream tree antennas. Even though the branch lengths and the number of branches are different than the Double version fractal trees, the far field patterns for the first frequency band is same. The other interesting point is that the patterns of Dream tree antennas are symmetric at the first and second band frequencies, although the geometry of the branches of the antennas is asymmetric.

The fractal tree antennas have same performance at various frequencies, so they behave like multiband antennas. Five frequency bands are observed for the fifth iteration of the Fibonacci and the Double version antennas. The antennas have same patterns at the first band frequency at each iterations, even though their resonance frequencies are different. The ripples in pattern figures are increasing at the higher band frequencies and the antennas are loosing the omnidirectional property. The fractal tree antennas show same behavior against various frequency bands. The main parameters derived from return loss figures are similar each other even though the branch lengths, number of branches and branch length ratios of the fractal tree antennas are different. The multiband behavior of the fractal tree antennas is consistent from the input return loss and radiation patterns points of view.

REFERENCES

[1] K. Falconer, "*Techniques in Fractal Geometry*", John Wiley&Sons Inc., Canada, (1997).

[2] M. F. Barnsley, "*Fractals Everywhere*," Academic Press Inc., Massachusetts, (1993).

[3] K. Falconer, "*Fractal Geometry Mathematical Foundations and Applications*," Wiley&Sons Inc., USA, (2002).

[4] J. P. Gianvittorio and Y. Rahmat Samii, "Fractal Antennas: A Novel Miniaturization Technique, and Applications," *IEEE Antennas and Propagat. Magazine*, vol.44, no. 1, February 2002, pp.20-36.

[5] C. Puente-Baliarda, J. Romeu, A. Cardama, "The Koch Monopole: A Small Fractal Antenna," *IEEE Trans. Antennas and Propagat*., vol.48, no.11, November 2000, pp.1773-1781.

[6] J. P. Gianvittorio and Y. Rahmat-Samii, "Fractal Element Antennas: A Compilation of Configurations with Novel Characteristics," *IEEE Antennas and Propagat. Soc. Int. Symp.*, vol.3, July 2000, pp. 1688-1691.

[7] C. Puente, J. Romeu, R. Pous, J. Ramis and A. Hijazo, "Small but long Koch fractal monopole," *Electronics Letters*, vol.34, no.1, January 1998, pp.9-10.

[8] C. Puente-Baliarda, J. Romeu, R. Pous, A. Cardama, "On the Behaviour of the Sierpinski Multiband Fractal Antenna," *IEEE Trans. Antennas and Propagat*., vol. 46, no.4, April 1998, pp. 517-524.

[9] C. Puente, J. Romeu, R. Pous, X. Garcia and F. Benitez, "Fractal Multiband antenna based on the Sierpinski gasket," *Electronics Letters*, vol.32, no.1, January 1996.

[10] C. Puente, J. Romeu, R. Bartoleme and R. Pous, "Perturbation of the Sierpinski antenna to allocate operating bands," *Electronics Letters*, vol. 32, no. 24, November 1996.

[11] J. Romeu and Jordi Soler, "Generalized Sierpinski Fractal Multiband Antenna," *IEEE Trans. on Antennas and Propagat*., vol.49, no.8, August 2001, pp.1237-1239.

[12] D. H. Werner, A. Rubio Bretones and B. R. Long, "Radiation characteristics of thin-wire ternary fractal trees," *Electronics Letters*, Vol. 35, No. 8, April 1999.

[13] S. R. Best, “On the Significance of Self-Similar Fractal Geometry in Determining the Multiband Behaviour of the Sierpinski Gasket Antenna,” *IEEE Antennas and Wireless Propagation Letters*, vol. 1, 2002, pp. 22-25.

[14] J. M. Gonzalez-Arbesu and J.Romeu, Size-reduction of pre-fractal Sierpinski monopole antenna, *Electronics Letters*, Vol.38, No.25, 2002, pp.1628-1630.

[15] C. Puente, J. Claret, F. Sagues, J. Romeu, M. Q. Lopez-Salvans and R.Pous, “Multiband properties of a fractal tree antenna generated by electrochemical deposition,” *Electronics Letters*, vol. 32, no.25, December 1996.

[16] M. Sindou, G. Ablart and C. Sourdois, “Multiband and wideband properties of printed fractal branched antennas,” *Electronics Letters*, vol. 35, no. 3, February 1999.

[17] S. R. Best, “On the Multiband behaviour of the Koch fractal monopole antenna,” *Microwave and Technology Letters*, vol. 35, no. 5, December 2002, pp. 371-374.

[18] S. R. Best, “A Discussion on the Significance of Geometry in Determining the Resonant Behavior of Fractal and Other Non-Euclidean Wire Antennas,” *IEEE Antennas and Propagat. Magazine*, vol.45, no.3, 2003, pp.9-28.

[19] S. R. Best, “The Effectiveness of Space-filling Fractal Geometry in Lowering Resonant Frequency,” *IEEE Antennas and Wireless Propagat. Letters*, vol.1, 2002, pp.112-115.

[20] K. J. Vinoy, K. A. Jose, V. K. Varadan, “On the Relationship between fractal dimension and the Performance of Multi-Resonant Dipole Antennas Using Koch Curves,” *IEEE Transactions on Antennas and Propagation*, vol. 51, no. 9, September 2003, pp. 2296-2303.

[21] K. J. Vinoy, J. K. Abraham and V. K. Varadan, “Fractal Dimension and Frequency Response of Fractal Shaped Antennas,” *in Proc. IEEE Antennas and Propagat. Soc. Int. Symp.*, Columbus, OH, USA, June 2003, pp.222-225.

[22] J. M. Gonzalez-Arbesu and J. Romeu, “Experiences on monopoles with the same fractal dimension and different topology,” *in Proc. IEEE Antennas and Propagat. Soc.*, vol.4, June 2003, pp.218-221.

[23] J. M. Gonzalez-Arbesu and J. Romeu, “On the influence of fractal dimension on radiation efficiency and quality factor of self-resonant prefractal wire monopoles”, *in Proc. IEEE Antennas and Propagat. Soc.*, vol.4, June 2003, pp. 214-217.

[24] J. M. Gonzalez-Arbesu, S. Blanch, J. Romeu, "Are Space-Filling Curves Efficient Small Antennas," *IEEE Antennas and Wireless Propagat. Letters*, vol.2, 2003, pp.147-150.

[25] R. F. Harrington, "Straight wires with arbitrarily excitation and loading," *IEEE Trans. on Antennas and Propagat.*, vol. AP-15, no.4, July 1967, pp.502-515.

[26] T. Koshy, *Fibonacci and Lucas Numbers with Applications*, Wiley&Sons Inc., USA, (2001).

[27] Supernec 2.7 Academic, Poynting Software Ltd., www.poynting.co.za.

[28] M. R. Donald, "The magical Fibonacci number," *Potentials, IEEE*, vol.9, issue:3, October 1990, pp.34-35.

[29] R. F. Harrington, *Field Computations by Moment Methods*, IEEE Press, (1993).

[30] W. Geyi, "Physical Limitations of Antenna," *IEEE Trans. On Antennas and Propagat.*, Vol. 51, 2003, pp.2116-2123.

[31] L. Fante, "Quality factor of General Ideal Antennas," *IEEE Trans. On Antennas and Propagat.*, AP-17, 1969, pp.151-155.

[32] C. A. Balanis, *Antenna Theory: Analysis and Design*, Wiley&Sons Inc., (1997).

[33] .J. D. Kraus, Antennas, McGraw-Hill Inc., (1988), Singapore.

[34] R. C. Johnson, *Antenna Engineering Handbook*, McGraw-Hill, Inc., (1993), USA.

[35] R. F. Harrington, *Time Harmonic Electromagnetic Fields*, John Wiley&Sons Inc., USA, (2001)

[36] J. S. Mclean, "A Re-Examination of the fundamental limits on the radiation Q of electrically small antennas," *IEEE Trans.on Antennas and Propagat*., vol.44, no.5, May 1996, pp. 672-676.

[37] http://www.jracademy.com/jtucek/math/uses.html, Friday, 16 July 2004, Time.15:47:12

[38] http://www.fractantenna.com, All pages © 1998-2004 Fractal Antenna Systems Inc.

[39] http://www.ee.ucla.edu/antlab